Check for updates

Flax lignan-fortified nanoemulsions potentiate the conversion of α-linolenic acid to n-3 LCPUFAs: cumulative metabolic patterns in non-fasting mice

Lei Wang,[a] Xiao Yu,*[a,b] Chen Cheng,[c] Jiqu Xu,[a] Xia Xiang, [ID][a] Li Chen,[a] Xiaoqiao Tang[d] and Qianchun Deng [ID]*[a]

As an essential n-3 fatty acid required by the human body, α-linolenic acid (ALA) can be metabolically converted *in vivo* into n-3 long chain polyunsaturated fatty acids (LCPUFAs) such as eicosapentaenoic acid (EPA) and docosahexaenoic acid (DHA), exhibiting biological functions and resource sustainability, and its conversion may be modulated by specific polyphenols. This study investigated the metabolic conversion profile in non-fasted mice following the intake of flaxseed oil nanoemulsions and assessed the potential regulatory effects of co-ingesting structurally distinct flax lignans. The results showed that co-administration of the flax lignan macromolecule (FLM) increased serum EPA by 31.9%, DHA by 20.2%, and hepatic EPA by 35.1%. Secoisolariciresinol diglucoside (SDG) increased serum EPA by 38% and hepatic EPA by 47.4%. Secoisolariciresinol (SECO) elevated serum EPA by 30.0%, and hepatic EPA, docosapentaenoic acid (DPA), and DHA by 57.9%, 19.7%, and 17.7%, respectively. Lipidomics revealed FLM/SECO enriched ALA-derived phospholipids (*e.g.*, PC 38:7|18:2_20:5), while SDG stimulated EPA/DHA-containing triglycerides (*e.g.*, TG 58:13|18:3_20:5_20:5), indicating lignan-specific effects. Furthermore, *in vivo* metabolic studies and HepG2 cell experiments indicated that the structural characteristics of flax lignans might determine their material basis of intestinal transport and hepatic metabolism, thereby modulating ALA absorption, transport, and conversion, with the characteristic metabolites SDG and enterodiol (ENL) further promoting downstream ALA-derived products (C20:4n-3, 48.6% or C20:3n-3, 48.1%), highlighting their regulatory roles. This study provides a theoretical foundation for developing functional lipid delivery systems based on lignan structural features and nutritional intervention strategies aimed at enhancing ALA metabolic conversion.

1. Introduction

N-3 long-chain polyunsaturated fatty acids (LCPUFAs), traditionally defined as those containing 20 or more carbon atoms with the first double bond positioned at the n-3 carbon, play crucial roles in maintaining human health by supporting physiological functions and preventing disease.[1,2] Seafood serves as their primary dietary source, but consumption is constrained by factors such as regional availability, resource limitations, marine environmental concerns, and cost.[3–5] Global surveys indicate that fewer than one-quarter of countries meet recommended n-3 LCPUFA intake levels from seafood, and approximately 100 countries, representing 66.8% of the world's adult population, have an average daily intake below 100 mg.[6] Consequently, identifying green, sustainable alternative dietary sources of n-3 LCPUFAs is urgent. Dietary supplementation with plant-derived α-linolenic acid (C18:3n-3, ALA), an essential fatty acid for humans, represents a promising strategy to alleviate this global insufficiency. ALA exerts significant health-promoting physiological effects and can be metabolically converted *in vivo* into eicosapentaenoic acid (C20:5n-3, EPA) and docosahexaenoic acid (C22:6n-3, DHA), enabling endogenous nutritional fortification.[7] Flaxseed, owing to its favorable ALA content and yield, is considered an excellent source for dietary ALA supplementation.[8] However, the efficacy of ALA intake faces significant bottlenecks, including susceptibility to gastrointestinal oxidation, inadequate

[a]*Oil Crops Research Institute of the Chinese Academy of Agricultural Sciences, Hubei Key Laboratory of Lipid Chemistry and Nutrition, and Key Laboratory of Oilseeds Processing, Ministry of Agriculture, Oil Crops and Lipids Process Technology National & Local Joint Engineering Laboratory, Wuhan 430062, Hubei, China. E-mail: dengqianchun@caas.cn; Fax: +86-27-86815916; Tel: +86-27-86827874*
[b]*College of Food and Bioengineering, Zhengzhou University of Light Industry, Zhengzhou 450001, Henan, China. E-mail: yuxiao@zzuli.edu.cn*
[c]*School of Modern Industry for Selenium Science and Engineering, Wuhan Polytechnic University, Wuhan 430023, Hubei, China*
[d]*Hubei Provincial Center of Disease Control and Prevention, Wuhan 430079, Hubei, China*

micellarization and absorption, and low metabolic conversion efficiency. These limitations consequently restrict the physiological availability of ALA substrates and impede the *in vivo* accumulation of its beneficial metabolites.[9]

The metabolic conversion of ALA to n-3 LCPUFAs is a sequential, multi-step process that alternates desaturation and elongation reactions within the endoplasmic reticulum, followed by partial β-oxidation in peroxisomes.[10] These reactions are catalyzed by Δ6-desaturase (FADS2), elongase of very long-chain fatty acids (ELOVL5), Δ5-desaturase (FADS1), and ELOVL2. Among these enzymes, Δ6-desaturase is widely regarded as the rate-limiting step in the pathway, exerting a major control over the metabolic flux from ALA to EPA and DHA. Within the elongation system, β-ketoacyl synthase (KAS) acts as the rate-limiting condensing enzyme that catalyzes the first step of each elongation cycle, which is the condensation of a long-chain acyl-CoA with malonyl-CoA to form β-ketoacyl-CoA, thereby determining the efficiency of chain elongation.[10] The liver is the principal site for these conversions, but extra-hepatic tissues, including the brain, testes, and kidneys, also exhibit measurable desaturase and elongase expression and activity, contributing to tissue-specific synthesis of n-3 LCPUFAs.[11] Additionally, nutritional factors such as the dietary n-6/n-3 ratio, micronutrient status (*e.g.*, zinc and iron), and hormonal cues (such as insulin-mediated SREBP-1c activation) can modulate the transcription and activity of FADS and ELOVL enzymes. Oxidative stress and metabolic disorders, including non-alcoholic fatty liver disease (NAFLD), further impair desaturase and elongase activities, resulting in reduced tissue n-3 PUFA biosynthesis.[10,12] Notably, serum-based measurements substantially underestimate whole-body DHA synthesis compared with integrative flux analyses (for example, approximately 0.2% *versus* 9.5% in mice, which represents about a 47-fold difference), highlighting the importance of tissue-specific regulation and the limitations of circulating biomarkers in assessing true conversion efficiency.[13] Given these complexities, a comprehensive understanding of dietary ALA supplementation necessitates investigating the factors governing its bioavailability, metabolic conversion, and tissue distribution. These encompass digestive and absorptive kinetics, tissue-specific conversion efficiency, the regulation of its metabolic partitioning (including synthesis, β-oxidation, and storage) by co-ingested bioactive compounds, as well as the influence of dietary composition, food matrix effects, and potential interactions with other nutritional constituents.

Compared to pure oil, protein, or Tween-stabilized emulsions, phospholipid-stabilized oil-in-water nanoemulsions offer advantages in enhancing the intestinal lipolysis, absorption, and transport rates of ALA.[14] Nevertheless, the significantly increased lipid droplet surface area in such nanoemulsions may exacerbate interfacial oxidation during digestion and increase the absorption of potentially harmful oxidation products.[15] Introducing specific polyphenols into nanoemulsion systems offers a potential solution. These compounds can improve the gastrointestinal oxidative stability of ALA and may achieve nutritional fortification by regulating the assembly

and transport of ALA-containing chylomicrons (CMs), hepatic metabolic allocation, and the expression of key converting enzymes.[9] Structure–activity relationships concerning existing research on modulating ALA conversion to n-3 LCPUFAs revealed key candidates, including curcumin,[16,17] resveratrol,[18] sesamol,[19,20] flax lignans,[21,22] quercetin,[23] fucoxanthin,[24,25] and anthocyanins,[26] which share core structural elements (phenolic hydroxyls, aromatic rings and conjugated systems) with distinct compound-specific features. Their potential regulatory targets are diverse, encompassing gastrointestinal digestive enzyme activity, ALA micellarization and intestinal absorption, hepatic expression of elongases/desaturases, and hepatic β-oxidation metabolism. Further assessment of the regulatory advantages and potential efficacy of relevant phenolic substances highlighted flax lignans. These compounds attracted particular attention due to their dual regulatory potential: as primary phenolic constituents in flaxseed hulls, they may enhance fatty acid uptake into hepatocytes, potentially promoting hepatic ALA transport and increasing substrate availability for conversion.[21] Additionally, they may regulate lipid metabolic distribution, potentially reducing ALA oxidative consumption and directing more substrates towards enhanced n-3 LCPUFA synthesis.[22] Furthermore, incorporating flax lignans into flaxseed oil nanoemulsion systems offers inherent natural homology advantages, forming a synergistic system. However, current research in this area predominantly relies on cell-based experiments, with regulatory mechanisms remaining unclear and insufficiently explored in depth.

Flax lignans primarily exist as oligomers of secoisolariciresinol diglucoside (SDG) concentrated in seed hulls, accompanied by minor amounts of matairesinol, pinoresinol, and isolariciresinol.[27] SDG mainly occurs as the conjugated diglucoside of secoisolariciresinol (SECO) and is ester-linked with 3-hydroxy-3-methylglutaric acid (HMGA) to form oligomeric macromolecules known as flax lignan macromolecule (FLM).[28,29] Preliminary laboratory studies found that natural FLM and its structural units (SDG and SECO) possess distinct antioxidant activities and interfacial properties, leading to differential effects on the gastrointestinal stability of nanoemulsions.[30] Simultaneously, flax lignans dose-dependently influence the digestion, absorption, and lymphatic/blood transport of ALA-containing lipids. Particularly, low-dose flax lignans enhance ALA bioavailability *via* a "rate decelerating but efficiency-enhancing" mechanism, potentially providing substrate availability for hepatic conversion of ALA to n-3 LCPUFAs.[31] Furthermore, compared to nanoemulsion intake alone, co-administration with flax lignans regulates hepatic ALA metabolic conversion in mice with "structure–activity differences", where FLM and SDG exhibit more pronounced positive regulatory effects.[32] However, a thought-provoking phenomenon was observed in the group administered with SECO-containing nanoemulsions: while it enhanced the expression of hepatic FADS and ELOVL in mice, it concurrently upregulated the rate-limiting enzyme for hepatic fatty acid β-oxidation, carnitine palmitoyltransferase (CPT1a). This finding strongly suggests that flax lignans may synchronously

regulate both the hepatic metabolic conversion of ALA and its subsequent metabolic partitioning. This raises a critical scientific question regarding whether, after long-term intake, the tissue fatty acid levels traditionally measured in the post-absorptive (fasted) state reflect the true conversion capacity or merely represent the net outcome masked by intense metabolic partitioning such as β-oxidation for energy. The inability to distinguish between these two scenarios hinders accurate assessment of the actual regulatory effects and mechanisms of different structural flax lignans, particularly the paradoxically behaving SECO.

Building on this foundation, the present study constructed flaxseed oil nanoemulsions incorporating structurally distinct flax lignans, using sunflower phospholipids as the emulsifier, and conducted long-term gavage experiments in mice. By quantitatively assessing the levels of ALA and n-3 LCPUFAs in the serum, liver, and peripheral tissues (including the adipose tissue and brain) under non-fasting conditions after the final administration, along with analyzing differences in serum lipid configurations mediated by hepatic uptake and secretion, the regulatory effects of flax lignans on ALA metabolic conversion were further elucidated. Simultaneously, the metabolic pathways and characteristic metabolites of lignans in the mouse liver were analyzed following a single gavage of lignan-flaxseed oil co-nanoemulsions. Furthermore, co-incubation experiments using HepG2 cells were performed with characteristic flax lignan metabolites and ALA to further clarify the potential material basis underlying lignan-mediated regulation of ALA metabolic conversion. Overall, this study aims to further elucidate the specific roles and mechanisms of flax lignans in regulating the *in vivo* metabolic conversion of ALA, as well as to identify the potential active substances involved, thereby providing theoretical support for dietary modulation of ALA metabolism *via* flaxseed oil nanoemulsions. The findings offer important evidence for optimizing dietary recommendations, supporting national nutrition policies, and guiding population-level interventions targeting n-3 LCPUFA deficiencies, while also contributing to the development of functional foods and sustainable dietary patterns aimed at improving global nutritional status and preventing chronic diseases associated with fatty acid deficiencies.

2. Materials and methods

2.1. Chemicals and reagents

Flaxseed oil was acquired from Hongjingyuan Oil Co., Ltd (Xilingol, Inner Mongolia, China). The flaxseed shell from the cultivar Longya no. 9 was generously provided by the Gansu Academy of Agricultural Sciences (Lanzhou, Gansu, China). Sunflower phospholipid PC90 (~90% phosphatidylcholine) and genistein were purchased from Macklin Biochemical Technology Co., Ltd (Shanghai, China). SDG (purity > 98%), SECO (purity > 98%), enterodiol (END, purity > 95%), and enterolactone (ENL, purity > 95%) were obtained from Yuanye Bio-Technology Co., Ltd (Shanghai, China). Methyl heptade-

canoate (purity > 99%) and ALA (purity > 99%) were sourced from Sigma-Aldrich (Saint Louis, MO, USA). A mixture of 37 fatty acid methyl ester standards was provided by ANPEL Laboratory Technologies Inc. (Shanghai, China), and the EquiSPLASH lipid standards mixture was obtained from Avanti Polar Lipids, Inc. (Alabaster, AL, USA). DMEM and fetal bovine serum were purchased from Gibco (Thermo Fisher Scientific, Carlsbad, CA, USA). Penicillin/streptomycin was acquired from Solarbio Science & Technology Co., Ltd (Beijing, China). Bovine serum albumin (fatty acid-free) was obtained from Yeasen Biotechnology Co., Ltd (Shanghai, China). Chromatographic-grade *n*-hexane, chloroform, dichloromethane, and acetonitrile were acquired from Merck KGaA (Darmstadt, Germany). Petroleum ether, ethanol, methanol, hydrochloric acid, diethyl ether, toluene, sulfuric acid, and other chemical reagents were procured from Sinopharm Chemical Reagent Co., Ltd (Beijing, China).

2.2. Preparation of sunflower phospholipid-stabilized water-in-flaxseed oil nanoemulsions

The extraction, purification, and purity determination of FLM and nanoemulsion preparation were performed as previously reported.[32] Briefly, sunflower phospholipids were dispersed and dissolved at 3% (w/w) in 5 mM phosphate-buffered saline (PBS, pH 7.0) to form the aqueous phase. FLM, SDG, and SECO were pre-dissolved in a minimal amount of 70% ethanol (v/v), and then mixed with the aqueous phase (80% w/w) and flaxseed oil (oil phase, 20% w/w). The final concentrations of SDG and SECO in the emulsion were 300 μmol L^{-1} each, while the FLM addition amount was calculated based on the equivalent SDG mass. Initially, coarse emulsion was obtained using a high-speed shear homogenizer (T25, IKA, Staufen, Germany) at 10 000 rpm for 2 min. Subsequently, the nanoemulsion was produced by processing through a high-pressure microfluidizer (M-110EH30, Microfluidics, Newton, MA) for four cycles at 10 000 psi.

2.3. Animal experiments

All animal protocols were approved by the Laboratory Animal Management and Use Committee of the Hubei Provincial Center for Disease Control and Prevention (approval no.: 202110106). Eight-week-old male C57BL/6J mice were supplied by the Experimental Animal Center of Hubei Province (license: SCXK-2020-0018) and Henan Skbex Biotechnology Co., Ltd (license: SCXK-2020-0005). Mice were housed in individually ventilated cages (6 mice per cage) under constant temperature (22 °C), constant humidity (40%–60%), and 12 h light/dark cycle conditions, with free access to feed and water. Customized standard diet (AIN93M) was provided by Trophic Animal Feed High-Tech Co., Ltd (Nantong, Jiangsu, China), and it contained casein, corn starch, corn dextrin, sucrose, cellulose, corn oil, methionine, choline bitartrate, vitamin mix, and mineral mix. Fatty acid composition of the diet determined by gas chromatography was: 12.5% palmitic acid (C16:0), 28.1% oleic acid (C18:1n-9), 57.3% linoleic acid (C18:2n-6, LA), and 0.8% ALA; fatty acid composition of flax-

seed oil was: 5.7% palmitic acid, 3.8% stearic acid (C18:0), 19.0% oleic acid, 16.2% LA, and 54.2% ALA.

2.4. Experimental procedure for apparent cumulative ALA absorption and conversion in the non-fasting state following the final gavage

Mice were randomly divided into 5 groups, with 18 mice per group and acclimated for one week. Subsequently, daily at 9:00 a.m., mice were administered by gavage: (1) control group (control): physiological saline; (2) nanoemulsion (NanoE); (3) FLM-containing nanoemulsion (FLM-N); (4) SDG-containing nanoemulsion (SDG-N); and (5) SECO-containing nanoemulsion (SECO-N). The gavage dose was 300 μL per mouse per day for 42 consecutive days, and changes in the body weight of the mice were recorded throughout the period (as shown in Fig. S1). Mice were euthanized in batches after 14, 28, and 42 days of gavage. Specifically, mice were fasted overnight (12 h), anesthetized with ether 6 h after the final gavage, and blood samples were collected. Subsequently, mice were euthanized by cervical dislocation, and the liver, adipose tissue, brain, small intestine, and other tissues were collected (the experimental procedure is illustrated in Fig. 1). Blood samples were centrifuged at 4000 rpm for 10 min at 4 °C to obtain the serum. Liver and other tissue samples were immediately snap-frozen in liquid nitrogen after collection and stored at −80 °C for further analysis.

2.5. Experimental procedure for lignan metabolism and hepatic transport following administration of flax lignan co-delivered nanoemulsions

Mice were randomly divided into four groups ($n = 20$ per group), with an additional five mice serving as the baseline group. Following one week of environmental acclimation and feeding on standard diet, mice were fasted for 12 h. The animals were administered by gavage: (1) nanoemulsion (NanoE); (2) FLM-containing nanoemulsion (FLM-N); (3) SDG-containing nanoemulsion (SDG-N); and (4) SECO-containing nanoemulsion (SECO-N) at a dose of 300 μL per mouse. Subsequently, at 1 h, 3 h, 6 h, 12 h, and 24 h post-gavage, mice were anesthetized with ether, blood samples were collected, and mice were euthanized by cervical dislocation. Tissue samples including those of the liver and small intestine were collected (the experimental procedure is shown in Fig. 6A). Serum samples were obtained by centrifugation at 4 °C and 4000 rpm for 10 min. Tissue samples were immediately snap-frozen in liquid nitrogen and stored at −80 °C for further analysis.

2.6. Determination of the fatty acid composition in serum and tissues

The fatty acid composition in the serum, liver, adipose tissue, and brain was measured according to previously described methods with slight modifications.[32] For serum samples, 100 μL was taken and mixed with 20 μL of an internal standard (methyl heptadecanoate, 5 mg mL^{-1} dissolved in petroleum ether), 2.0 mL of sulfuric acid–methanol solution (5%, v/v), and 300 μL of toluene, and placed into a 10 mL screw-cap glass tube. The mixture was then incubated at 95 °C for 90 min in a water bath, with manual shaking for 10 s every 30 min. After cooling to room temperature, 2.0 mL of physiological saline and 1.0 mL of n-hexane were added, vortex-mixed for 3 min, and allowed to stand for 10 min before centrifugation at 4000 rpm for 10 min. The upper organic phase was carefully transferred to another test tube, evaporated to dryness under nitrogen gas, reconstituted in 200 μL of n-hexane, filtered through a 0.22 μm membrane, and then analyzed. Tissue samples, after adding the internal standard, underwent lipid extraction using a chloroform/methanol solu-
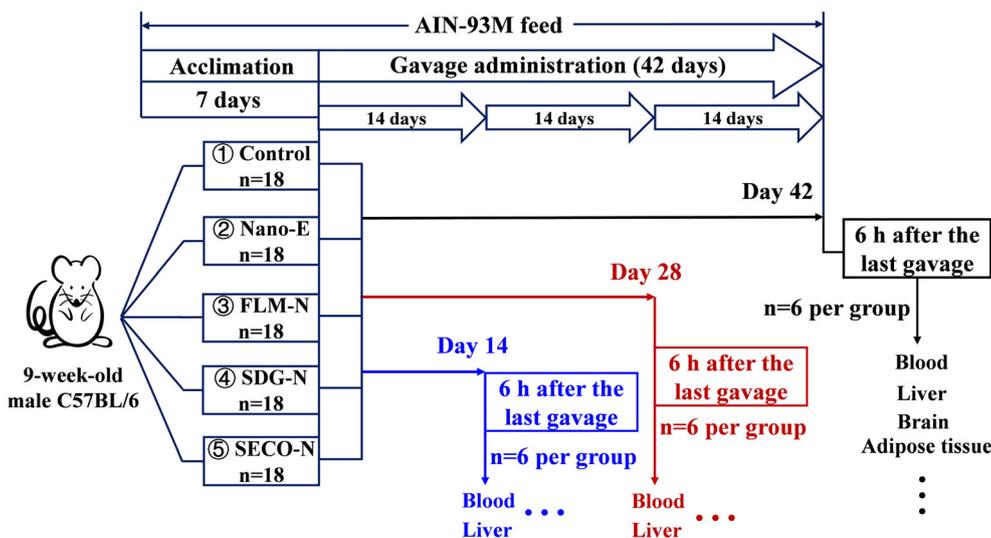

Fig. 1 Experimental procedure diagram for investigating the cumulative effects of ALA absorption and conversion in mice under non-fasting conditions.

tion. The extracted lipid phase was dried under nitrogen gas before the subsequent methylation procedures.[33]

Fatty acid methyl esters (FAMEs) were analyzed by gas chromatography (7890A, Agilent Technologies, California, USA) equipped with a capillary column (HP-FFAP, 30 m × 0.25 mm × 0.25 μm, Agilent) and a flame ionization detector (FID). The initial oven temperature was set at 130 °C and held for 3 min, then increased to 200 °C at 5 °C min^{-1} and held for 10 min, and finally raised to 220 °C at 2 °C min^{-1} and held for 3 min. The injector and detector temperatures were controlled at 250 °C and 280 °C, respectively. The nitrogen flow rate was 1.8 mL min^{-1}, the split ratio was adjusted according to the lipid content in different samples, and the injection volume was 2 μL.

2.7. Determination of the serum lipid configuration

The determination of the serum lipid configuration followed the method previously described by Wang *et al.*, with minor modifications.[34] Briefly, 100 mg of serum sample was weighed into a 16 mL glass culture tube, to which 10 μL of an internal standard solution (10 μg mL^{-1}) was added, followed by sequential addition of 2 mL of methanol and 2 mL of dichloromethane, vortexing for extraction over 30 min. Subsequently, 2 mL of dichloromethane and 1.6 mL of ultrapure water were added, vortex-mixed for an additional 10 min, and centrifuged at 4000 rpm. The lower clear layer was collected. The upper layer was re-extracted twice with 4 mL of dichloromethane each time. All lower layers were combined, evaporated under a nitrogen stream, reconstituted with 150 μL of chloroform/methanol (v/v, 2 : 1) and filtered through a 0.22 μm organic membrane, and then injected for analysis. Lipid separation was performed using an ultra-performance liquid chromatography (UPLC, Nexera X2, Shimadzu, Kyoto, Japan) system equipped with a Phenomenex Kinetex C18 column (100 mm × 2.1 mm, 2.6 μm). Mobile phase A consisted of H$_2$O/MeOH/ACN (1 : 1 : 1, v/v, containing 5 mM NH$_4$AC) and mobile phase B was IPA/ACN (5 : 1, v/v, containing 5 mM NH$_4$AC). The flow rate was 0.4 mL min^{-1} with a column temperature of 60 °C; the sample tray and injector were maintained at 4 °C. Injection volumes were 2 μL for the positive ion mode and 6 μL for the negative ion mode. The gradient elution program was as follows: 0–0.5 min, 20% B; 0.5–1.5 min, 20–40% B; 1.5–3.0 min, 40–60% B; 3.0–13.0 min, 60–98% B; 13.0–13.1 min, 98–20% B; 13.1–17.0 min, 20% B. Mass spectrometric detection was carried out using a quadrupole time-of-flight tandem mass spectrometer (Triple TOF 6600 plus, AB Sciex, Framingham, MA, USA). Primary scanning ranged from *m/z* 100–1200 Da and secondary scanning from *m/z* 50–1200 Da in both positive and negative ion modes. Declustering potential (DP) was set at 80 V (+) and −80 V (−); collision energy (CE) was 10 V (+) and −30 V (−); and ion spray voltage floating (ISVF) was 5500 V (+) and −4500 V (−). Nebulizer gas (GS1) and heater gas (GS2) were both 50 psi; curtain gas (CUR) was 35 psi; and the ion source temperature was set at 600 °C, with nitrogen as the nebulizing and auxiliary gas.

LC-MS raw data files (.wiff) were converted into MS-DIAL analysis files (.abf). Lipid identification was preliminarily performed by using MS-DIAL software using the Lipid Blast database for peak searching, alignment, and annotation. To improve accuracy and avoid false positives, PeakView software was used for manual verification, strictly screening and confirming results based on three criteria: molecular mass (error < 5 ppm), retention time (error < 5%), and isotopic pattern (error < 10%). Subsequently, Masterview software was employed to establish quantitative methods using lipid names, retention times (RT), and mass-to-charge ratios (*m/z*). Finally, Multiquant software was used to integrate lipid peak areas, with quantitative analysis of identified serum lipid molecules performed using the internal standard method.

2.8. Identification and quantitative analysis of flax lignans and metabolites in the liver

The analysis of flax lignans and metabolites in the liver was performed following the methods of Bolca *et al.* and García-Mateos *et al.*, with modifications.[35,36] First, a genistein internal standard solution was prepared by dissolving 5 mg in 4 mL of methanol to obtain a stock solution, which was subsequently diluted 50-fold to prepare a working solution. Subsequently, 250 mg of liver tissue was weighed into a 2 mL centrifuge tube, and the internal standard (20 μL) was added, followed by 1 mL of methanol/water (8 : 2, v/v) containing 200 mM hydrochloric acid. The mixture was homogenized and ground for 2 min (two times, each for 1 min), and then transferred into a 10 mL high-speed centrifuge tube. An additional 4 mL of the same buffer solution was used for rinsing and combined with the homogenate. The supernatant was collected, concentrated under a nitrogen stream, transferred to a 2 mL centrifuge tube, evaporated to dryness under nitrogen, reconstituted with 250 μL of methanol, filtered through a 0.22 μm membrane, and injected for analysis.

Lignan metabolites were detected using a UPLC-qTOF-MS system (Agilent 1290 UPLC coupled with 6550 Q-TOFMS) with a Waters BEH C18 column (2.1 × 100 mm, 1.7 μm). The mobile phases consisted of water containing 0.1% formic acid (A) and acetonitrile (B). The gradient elution program was: 0–10 min, 5–25% B; 10–20 min, 25–40% B; 20–24 min, 40–90% B; then returning to 5% B and equilibrating for 4 min. The flow rate was 0.3 mL min^{-1}, and the injection volume was 5 μL.

2.9. *In vitro* co-incubation experiment of the characteristic flax lignan metabolites and ALA in HepG2 cells

The HepG2 cell co-incubation experiment was designed with reference to previously described methods with minor modifications.[18,37] Human hepatocellular carcinoma HepG2 cells, supplied by Procell Life Science & Technology Co., Ltd (Wuhan, Hubei, China), were cultured in DMEM containing 10% (v/v) fetal bovine serum and 1% penicillin/streptomycin in a humidified incubator at 37 °C with 5% CO$_2$. Experimental procedures commenced when cells reached approximately 80% confluence, ensuring that the concentrations of lignans (SDG, SECO, END, and ENL) and ALA used were within non-

toxic ranges. The preparation for the ALA–BSA complex was as follows: ALA stock solution was prepared by dissolving ALA in 1 M NaOH solution and vortexing for 10 min; separately, FFA-free BSA was dissolved in serum-free DMEM. The ALA stock solution was then added dropwise to the BSA solution, vortexed for 10 min, purged with nitrogen, and incubated at 37 °C in a shaker for 2 h. Subsequently, the mixture was filtered through a 0.22 μm membrane to obtain the ALA–BSA complex at a molar ratio of 3 : 1 (final concentrations: ALA – 1 mM and BSA – 0.33 mM). Flax lignan stock solutions were initially dissolved in DMSO and added to the culture medium at appropriate ratios in the experiments; the control group received an equivalent volume of DMSO solution. HepG2 cells were cultured separately in DMEM containing ALA (100 μM) and different flax lignans (100 μM) for 48 h. Subsequently, cells and the culture medium were collected for lipid extraction, followed by further determination and analysis of the fatty acid content.

2.10. Qualitative and quantitative analyses of fatty acids in the cell experiment samples

Gas chromatography-mass spectrometry (GC-MS, Agilent 7890A-5975C) was employed for the qualitative and quantitative analyses of fatty acids extracted and methylated from the cell or culture medium samples. Sample pretreatment for methylation was performed as described in section 2.6. The chromatographic column used was a DB-WAX column (30.0 m × 250 μm, 0.25 μm); the initial temperature was set at 100 °C and held for 5 min, and then increased to 240 °C at 8 °C min^{-1} and held for 20 min. The injector temperature was set at 250 °C, the transfer line temperature was 240 °C, helium was utilized as the carrier gas at a flow rate of 1.0 mL min^{-1}, the split ratio was 10 : 1, and the injection volume was 1 μL. The mass spectrometry conditions were as follows: electron ionization (EI) source; electron energy at 70 eV; ion source temperature at 230 °C; quadrupole temperature at 150 °C; scan mode; mass scan range of 33–500 u; and a solvent delay of 3 min.

2.11. Data analysis

The results were expressed as mean ± standard deviation (mean ± SD). Data analysis was performed using SPSS software (V20, SPSS Inc., USA). One-way analysis of variance (ANOVA) followed by Duncan's multiple comparison test (Duncan's test) was employed to determine the significant differences among the sample groups. A p-value less than 0.05 ($p < 0.05$) was considered statistically significant.

3. Results and discussion

3.1. Time-cumulative effects of ALA absorption–conversion in the serum and liver

In our previous report, the basic physical characteristics of the emulsions currently used were described, including particle size, zeta potential, microstructure, and TSI stability. The results showed that the particle size of the coarse emulsion without microfluidization treatment was approximately 7.68 μm, while nanoemulsions in all groups ranged from 226 to 263 nm; the addition of flax lignans did not significantly affect the physical stability of the nanoemulsions (Table S1 and Fig. S2).[31]

Based on this established stable nanoemulsion system, the present study investigated the time-dependent effects of co-ingesting lignans (FLM, SDG, or SECO) on the serum levels of ALA, EPA, docosapentaenoic acid (C22:5n-3, DPA), and DHA in mice gavaged with nanoemulsions. As shown in Fig. 2A–D, compared to the control group, intake of Nano-E significantly increased the serum ALA content at all time points and further elevated its conversion into EPA, DPA, and DHA, implying that mice were unable to synthesize ALA endogenously and required exogenous supplementation. In the Nano-E group, the intestinal absorption, hepatic uptake, and secretion of ALA induced dynamic changes in the serum levels. The ALA content peaked at day 14, slightly declined at day 28, and then modestly rebounded at day 42. This observed decline in the serum ALA content may relate to real-time hepatic accumulation and enhanced conversion metabolism. Compared with Nano-E, lignan co-intake caused temporal fluctuations in ALA content, but without significant changes. Serum EPA levels showed limited cumulative effects over time, with minimal overall variations. The elevated serum EPA levels observed in the Nano-E group at day 28 might relate to enhanced concurrent conversion, corresponding to the reduction in serum ALA. Meanwhile, serum DPA content showed obvious time-cumulative effects, particularly in the FLM-N and SDG-N groups, displaying continuous and steady increases. In contrast, serum DHA levels remained relatively stable throughout the experiment, with only the FLM-N group showing a slight upward trend, suggesting that FLM exerts time-cumulative regulatory effects on the ALA to DHA conversion. Notably, previous studies showed that under moderate flaxseed diets, the *in vivo* content of ALA and its conversion products (*e.g.*, EPA, DPA and DHA) gradually increased over time (0–15–30 days), while whole-body retention and apparent conversion rates gradually decreased, and oxidative metabolic rates progressively increased.[38] Simultaneously, other studies indicated that increasing dietary ALA content (1%–5%) gradually elevated ALA and n-3 LCPUFA levels in mice, but higher ALA doses (7.5%) or co-intake of EPA (0.25%–1%) may reduce the conversion efficiency of ALA to n-3 LCPUFAs through substrate inhibition.[39] Combining with the current results, the decreased EPA content in the Nano-E group at day 42 may result from product inhibition, while co-ingestion of lignans may mitigate adverse impacts by slowing ALA absorption–transport rates, thereby reducing the real-time metabolic rate in the liver.

Additionally, the time-dependent effects of co-intake flax lignans (FLM, SDG, or SECO) on the hepatic levels of ALA, EPA, DPA, and DHA in mice gavaged with nanoemulsions were investigated over time. As shown in Fig. 2E–H, compared with the control, intake of Nano-E significantly increased the hepatic ALA content at each time point and further elevated
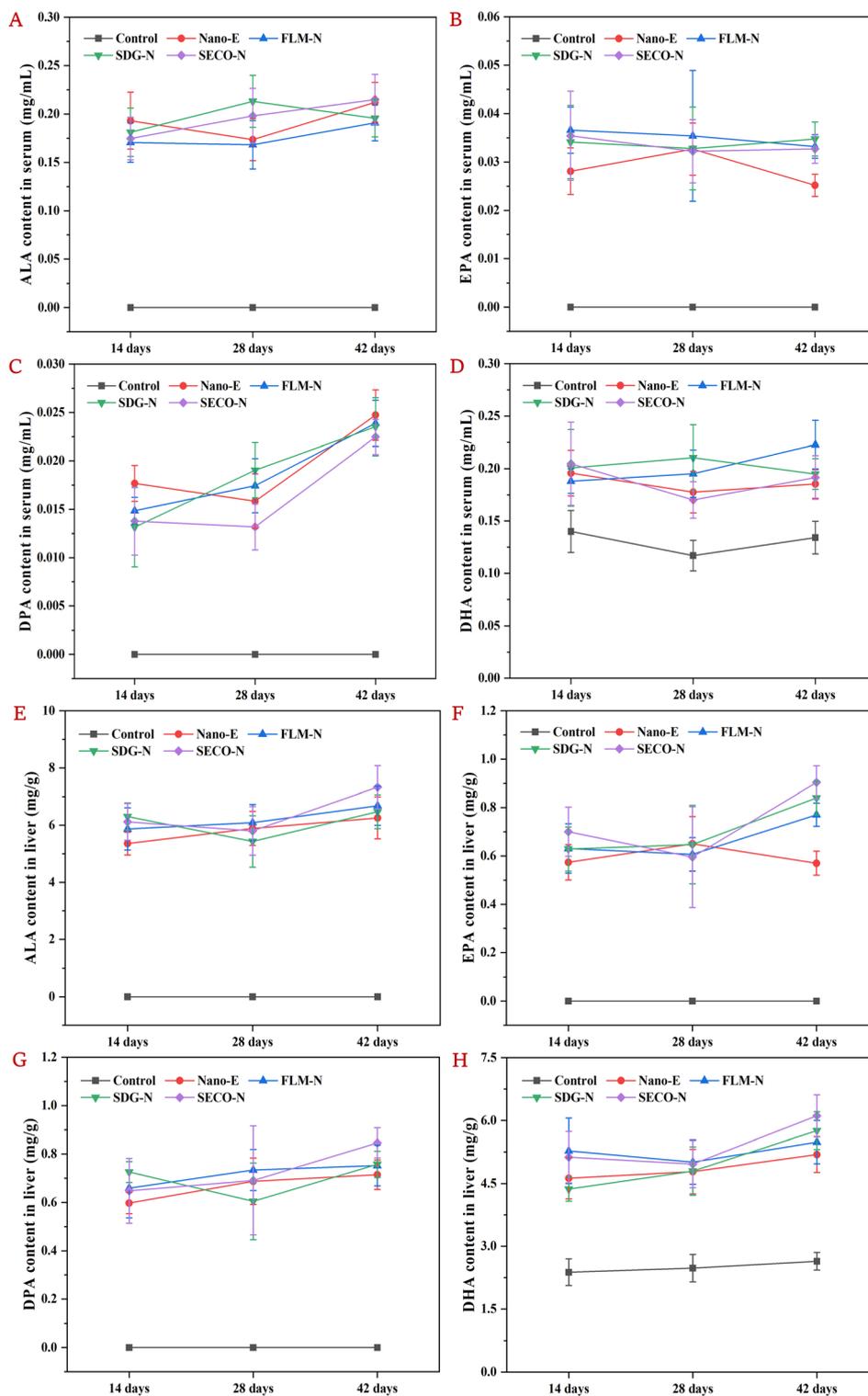
Fig. 2 Time-accumulated effects of ALA absorption–conversion in the serum and liver 6 h after the final intragastric administration on days 14, 28, and 42. (A–D) Changes in the ALA, EPA, DPA, and DHA contents in the serum and (E–H) changes in the ALA, EPA, DPA, and DHA contents in the liver.

the EPA, DPA, and DHA content. In the NanoE group, hepatic ALA uptake exhibited a slight increasing trend. Co-intake of SDG or SECO resulted in reduced hepatic ALA content at day 28, possibly relating to real-time serum secretion and enhanced conversion metabolism. For hepatic EPA, the FLM-N, SDG-N, and SECO-N groups, all exhibited upward

trends, demonstrating time-cumulative enhancement effects on the ALA metabolic conversion. The decreased hepatic EPA content in the Nano-E group at day 42 may result from reduced ALA uptake and simultaneous enhancement in DPA and DHA conversion. Meanwhile, slower intestinal absorption and hepatic transport induced by lignan co-intake may alleviate negative feedback inhibition effects caused by hepatic conversion products. In contrast, hepatic DPA levels fluctuated slightly over time but maintained a steady increase in the FLM-N and SECO-N groups. Similarly, hepatic DHA levels showed no significant fluctuations at days 14 and 28 but modest increases at day 42, particularly in the SDG-N and SECO-N groups. These results indicated that FLM, SDG, or SECO all possess time-cumulative regulatory effects on enhan-

cing ALA conversion to n-3 LCPUFAs, suggesting that they may contain material basis components that promote the ALA metabolic conversion.

3.2. Differential regulation of flax lignans on serum and hepatic n-3 PUFA contents in non-fasted mice

Subsequently, the analysis of the fatty acid composition and the quantified n-3 PUFAs in the sera and livers of mice 6 h after the last gavage at day 42 was conducted. As shown in Fig. 3A–E, significant differences were observed in the percentage composition of serum fatty acids among the different experimental groups. Oleic acid (C18:1n-9) was the predominant fatty acid in the serum across the groups, accounting for
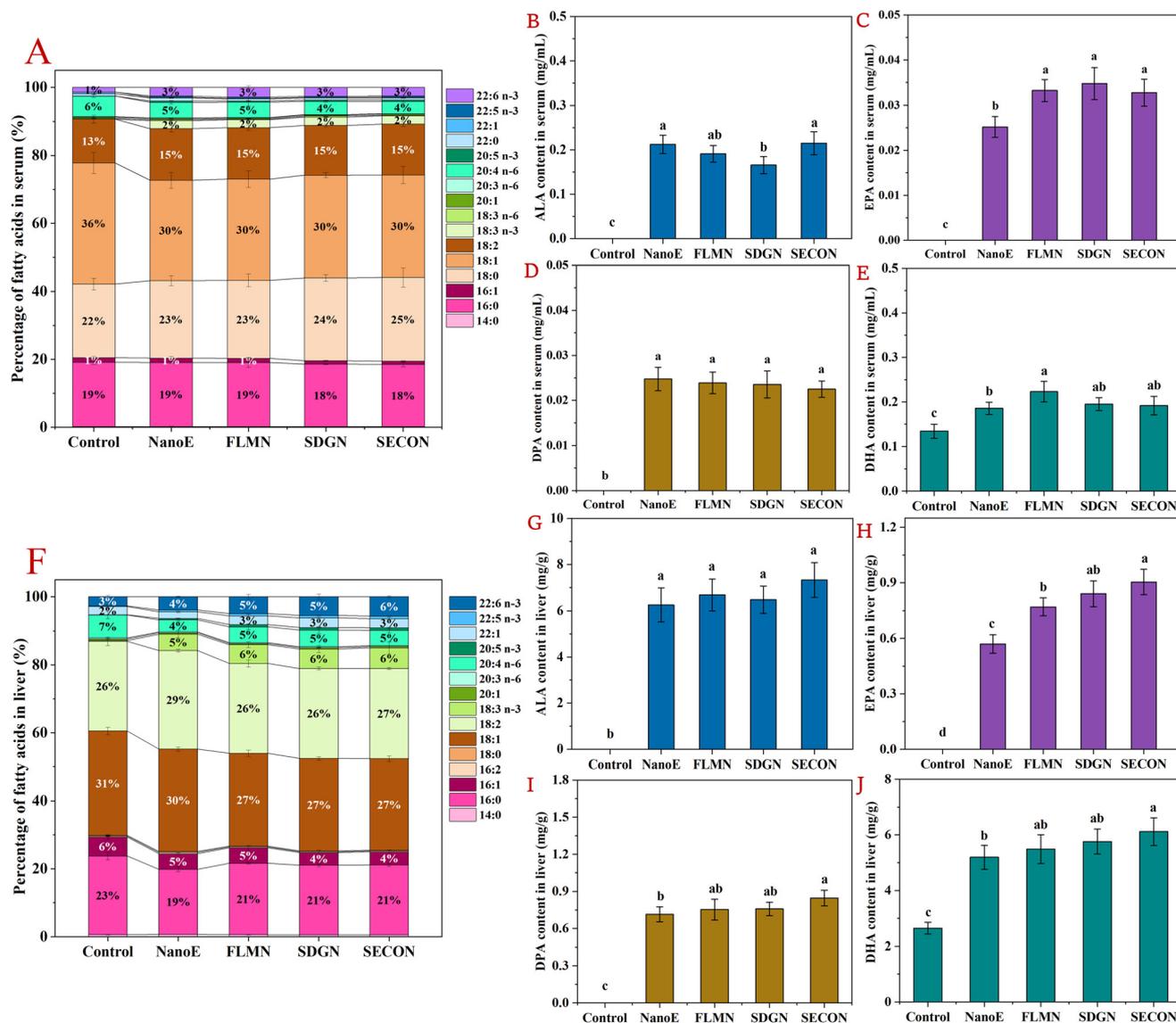

Fig. 3 Quantitative analysis of the fatty acid composition and n-3 PUFAs in the sera and livers of mice 6 h after the final intragastric administration over 42 days. (A–E) Percentage composition of fatty acids, and the levels of ALA, EPA, DPA, and DHA in the serum. (F–J) Percentage composition of fatty acids, and the levels of ALA, EPA, DPA, and DHA in the liver.

approximately 29%–36%, followed by stearic acid (C18:0, 22%–25%), palmitic acid (C16:0, 18%–19%), LA (13%–15%), and arachidonic acid (C20:4n-6, AA, 4%–6%). Compared with the control group gavaged with physiological saline, nanoemulsion intake increased the serum ALA proportion from 0% to 2% and the DHA proportion from 1% to 3%. Simultaneously, AA proportion decreased from 6% to 4%–5%. Quantitative analysis of serum n-3 PUFAs revealed significant differences in the ALA, EPA, DPA, and DHA levels among the groups. Specifically, ALA, EPA, and DPA were undetectable in the serum of control group mice, while DHA levels were 0.13 mg mL^{-1}. In contrast, n-3 PUFA levels significantly increased in all nanoemulsion-gavaged groups, with the NanoE group showing ALA, EPA, and DPA levels of 0.21 mg mL^{-1}, 0.025 mg mL^{-1}, and 0.025 mg mL^{-1}, respectively, and DHA levels further increasing to 0.19 mg mL^{-1}. Furthermore, compared with the NanoE group, serum EPA (+31.9%) and DHA (+20.2%) levels were significantly elevated in the FLM-N group ($p < 0.05$), indicating that co-administration of FLM has certain advantages in promoting the hepatic conversion of ALA and lipoprotein secretion. In comparison, co-intake of SDG or SECO increased serum EPA levels by 30.0%–38.0%, without significantly altering the DPA or DHA levels, showing that SDG and SECO also exhibit regulatory effects in promoting the ALA metabolic conversion.

As shown in Fig. 3F–J, the major hepatic fatty acids across the groups were oleic acid (C18:1), accounting for 27%–31%, followed by LA (26%–29%), palmitic acid (C16:0, 19%–23%), AA (4%–7%), and palmitoleic acid (C16:1n7, 4%–6%). Compared with the control group, nanoemulsion intake significantly increased the hepatic ALA proportion from 0% to 5%–6% and the DHA proportion from 3% to 4%–6%, while decreasing the AA proportion from 7% to 4%–5%. Similarly, quantitative analysis showed lower hepatic levels of ALA, EPA, and DPA in the control group, with DHA at 2.64 mg g^{-1}. In contrast, the nanoemulsion-gavaged groups exhibited significantly elevated hepatic n-3 PUFA content, with the NanoE group showing ALA, EPA, and DPA contents elevated to 6.26 mg mL^{-1}, 0.57 mg mL^{-1}, and 0.71 mg mL^{-1}, respectively, and DHA content further increased to 5.19 mg mL^{-1}. Additionally, compared with the NanoE group, co-intake of FLM or SDG further increased hepatic EPA levels (+35.1%–47.4%), whereas SECO co-intake simultaneously elevated EPA (+57.9%), DPA (+19.7%), and DHA (+17.7%) levels, exhibiting regulatory effects in enhancing ALA conversion to n-3 LCPUFAs. Our previous research also showed that co-administration of SDG-containing nanoemulsions increased hepatic EPA and DHA levels by 10%–13% in fasted mice. Furthermore, combined intake of FLM and SDG elevated serum EPA concentrations by 52.7%–55.9%, indicating a positive regulatory effect of flax lignans on the metabolic conversion of ALA into n-3 LCPUFAs.[32]

3.3. Effects of flax lignans on the n-3 PUFA content in the brains and adipose tissue of non-fasted mice

As shown in Fig. 4A–C, the fatty acid composition in the brain tissue remained relatively stable across all experimental groups, with major fatty acids including saturated fatty acids (C16:0 and C18:0) collectively accounting for ~39%, mono-unsaturated fatty acids (C18:1n-9) comprising ~20%, and AA constituting ~9%. After ingestion of flaxseed oil nanoemulsion, ALA was undetectable in brain tissue, indicating its inability to cross the blood–brain barrier. Compared with the control group, all nanoemulsion-gavaged groups showed modest increases in brain DHA (18% → 19%). Overall, nanoemulsion intake exerted limited effects on the brain fatty acid composition. Quantitative analysis revealed that compared with the control group, nanoemulsion intake significantly increased the brain EPA levels (0 → 0.1 mg g^{-1}), but no significant differences existed among the groups co-administered lignan-containing nanoemulsions. Simultaneously, the brain DHA levels significantly increased in the nanoemulsion groups (6.2 → 6.58–6.74 mg g^{-1}) compared with the control group, but lignan co-intake had no significant effect. These results indicated that ingestion of nanoemulsion significantly elevated the brain n-3 PUFA content in mice, whereas lignan co-administration had limited effects on increasing the brain n-3 PUFA levels.

As shown in Fig. 4D–H, major fatty acids in adipose tissue across the groups were oleic acid (38%–40%), LA (32%–34%), palmitic acid (15%–17%), and palmitoleic acid (5%–6%). Compared with the control group, nanoemulsion intake significantly increased adipose ALA proportion (0% → 3%), while percentages of other fatty acids remained stable. Quantitative analysis revealed low adipose tissue levels of ALA, EPA, DPA, and DHA in the control mice, with DHA at 0.65 mg g^{-1}. In contrast, the nanoemulsion-gavaged groups exhibited significantly elevated n-3 PUFA levels, with ALA, EPA, DPA, and DHA increasing to 22.1, 0.38, 1.26, and 1.95 mg g^{-1}, respectively. Previous studies reported significant increases in the adipose tissue levels of ALA, EPA, and DHA and a reduction in the n-6/n-3 ratio following dietary administration of ALA-rich chia seed oil in rats.[40] Compared with the NanoE group, FLM-containing nanoemulsion further increased the adipose EPA levels (+23.7%) without significantly altering other n-3 PUFA levels. Conversely, co-intake of SDG- or SECO-containing nanoemulsions elevated adipose ALA levels by 14%, without affecting EPA, DPA, or DHA levels.

3.4. Lipidomic analysis of n-3 PUFA configurations in the sera of non-fasted mice

Serum lipid profiles of mice administered saline (control), nanoemulsion (NanoE), FLM-containing nanoemulsion (FLM-N), SDG-containing nanoemulsion (SDG-N), and SECO-containing nanoemulsion (SECO-N) were quantitatively analyzed using UPLC-Q-TOF-MS, with a focus on the configuration and content changes of n-3 PUFA-containing lipids in the emulsion groups. Lipidomic analysis identified 213 lipid species based on internal standard quantification, encompassing lipid classes including cholesteryl ester (CE, 8 species), ceramide (Cer, 2), diacylglycerol (DG, 22), lyso-phosphatidylcholine (LPC, 15), phosphatidylcholine (PC, 28), sphingomyelin (SM, 10), TG (triacylglycerol, 79), FA (fatty acid, 21), LPE (lyso-
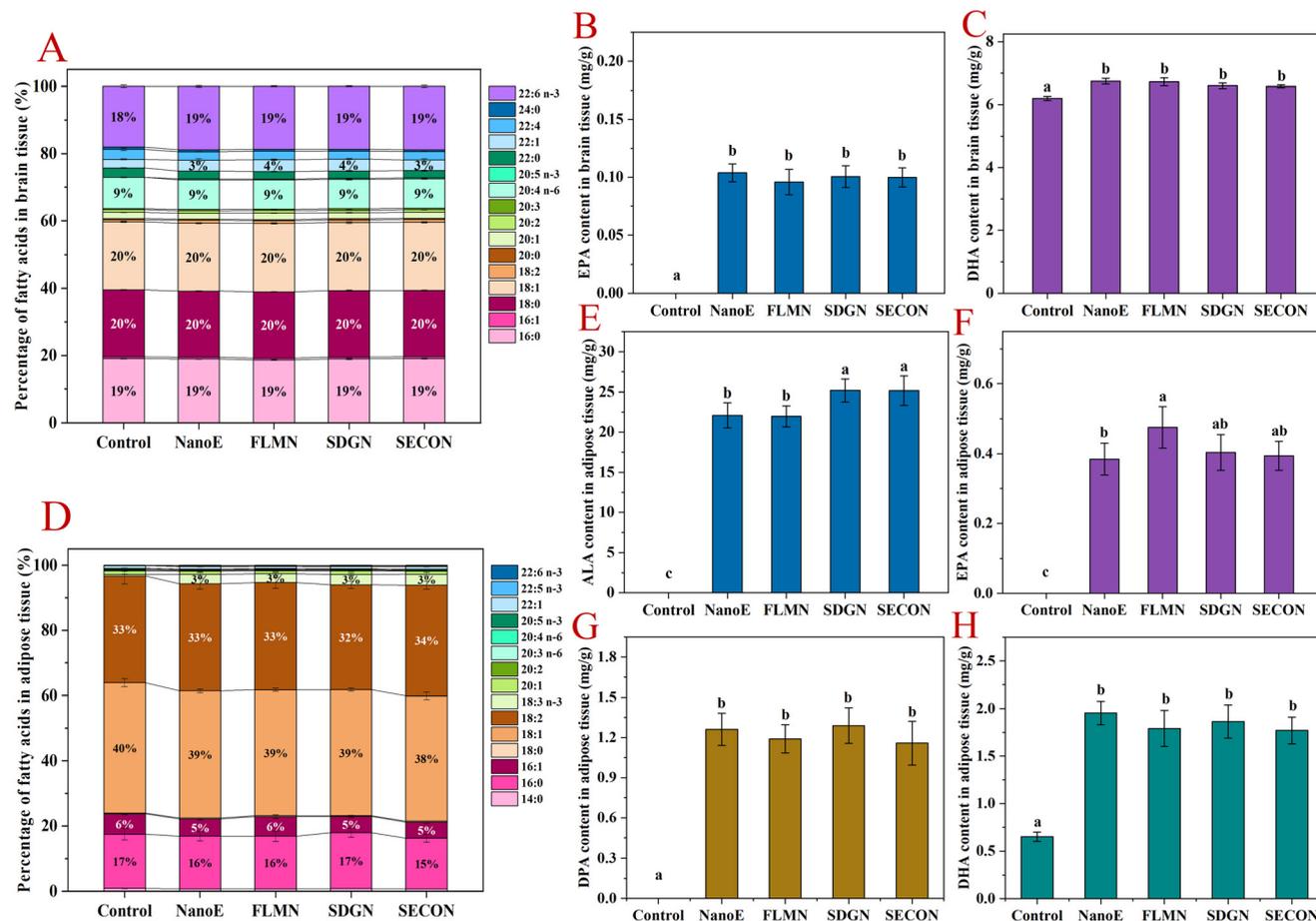
Fig. 4 Quantitative analysis of the fatty acid composition and n-3 PUFAs in the brains and adipose tissues of mice 6 h after the final intragastric administration over 42 days. (A–C) Percentage composition of fatty acids, and the levels of EPA and DHA in the brain. (D–H) Percentage composition of fatty acids, and the levels of ALA, EPA, DPA, and DHA in the adipose tissue.

phosphatidylethanolamine, 6), PA (phosphatidic acid, 4), PE (phosphatidylethanolamine, 11), and PI (phosphatidylinositol, 7). Further focusing on n-3 PUFA-containing lipids, 61 lipid species were identified, involving CE (3), DG (5), FA (4), LPC (4), LPE (2), PC (10), PE (2), PI (1), and TG (30). Fig. 5A shows the heatmap analysis of serum n-3 PUFA-containing lipids across the groups. Control group lipid levels were generally low, while nanoemulsion intake increased the abundance of multiple lipid configurations, showing elevated (red) patterns. Compared with the NanoE group, co-intake of FLM-, SDG-, or SECO-containing nanoemulsions further elevated multiple lipid configurations, particularly enriching TG and PC lipids, indicated by intensified red regions. Simultaneously, dendrogram clustering analysis (left of the heatmap) clearly distinguished the control group from all nanoemulsion groups, suggesting that nanoemulsion administration significantly altered serum lipid composition in the mice. The FLM-N, SDG-N, and SECO-N groups clustered more closely than the NanoE group, indicating similarity in lipidomic regulatory effects, implying potential overlap in the action targets of different flax lignans on n-3 lipid metabolic conversion.

Configuration distribution based on the quantitative results of n-3 PUFA-containing lipids is shown in Fig. 5B. In the NanoE group, TG accounted for the highest proportion (44.94%), followed by FA (28.56%) and PC (19.59%). Compared with the Nano-E group, the FLM-N group showed reduced TG proportion (39.38%), but increased PC proportion (24.32%) and slightly decreased FA proportion (27.88%). Furthermore, the SDG-N group had TG proportion at 40.26%, increased PC proportion (24.07%), the highest LPC proportion (6.15%), and slightly increased LPE proportion (1.87%). In contrast, the SECO-N group exhibited the lowest TG proportion (38.57%), highest FA proportion (32.80%) and relatively high PC proportion (22.06%), but lower LPC (4.78%) and LPE (1.15%) proportions. Additionally, DG, PE, PI, and CE proportions were low or negligible in all groups (<1%). Therefore, lignan co-intake significantly influenced the configuration distribution of serum n-3 PUFA-containing lipids, particularly affecting the proportions of TG, PC, and FA lipids.

Volcano plot analysis of differences in n-3 PUFA-containing lipids among the groups is shown in Fig. 5C. Each point represents a specific lipid configuration, with red indicating signifi-
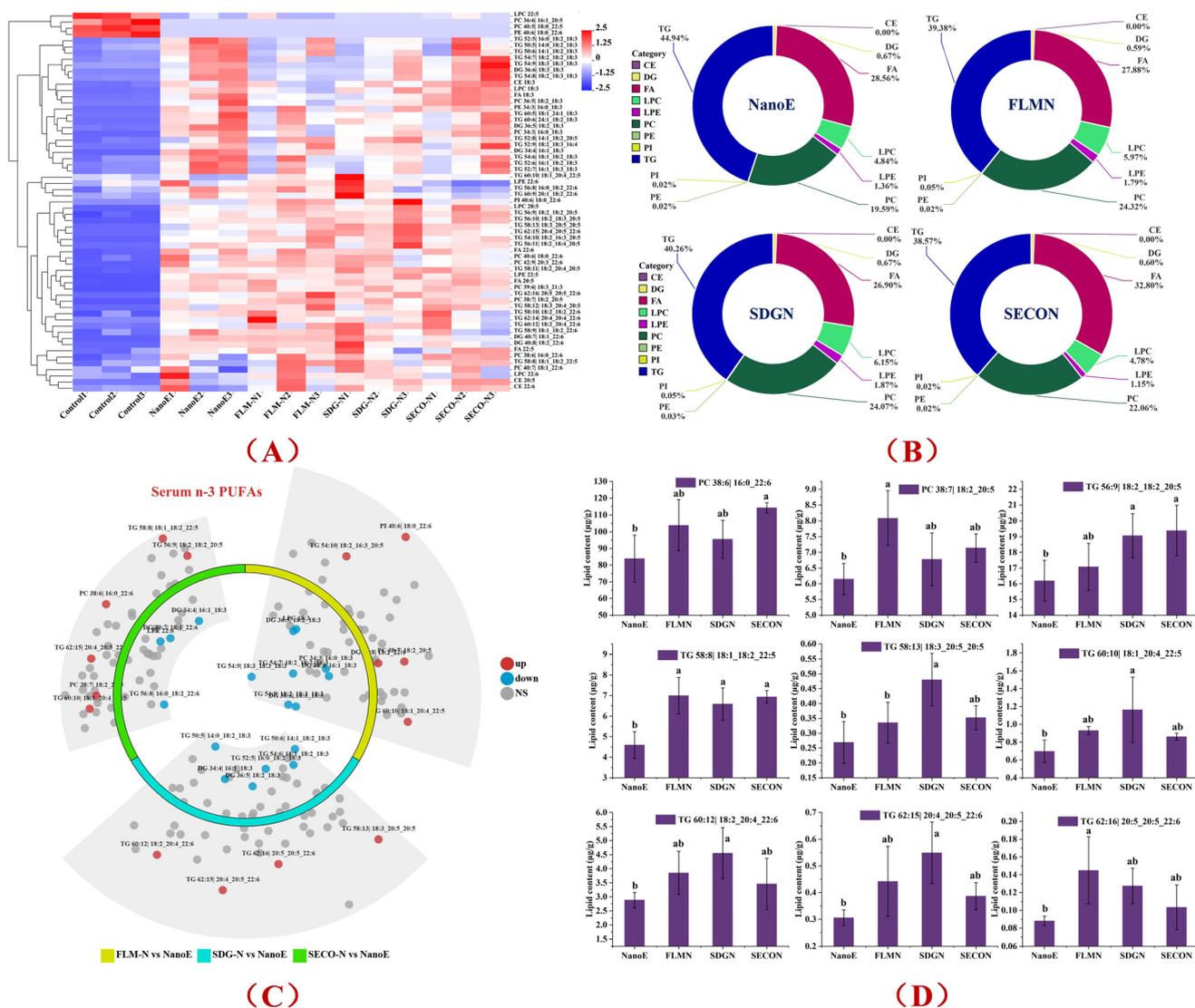
Fig. 5 Analysis of serum n-3 PUFA configurations in mice 6 h after the final intragastric administration over 42 days. (A) Heatmap analysis of n-3 PUFA-containing lipids; (B) configuration distribution of n-3 PUFA-containing lipids; (C) volcano plot of differential n-3 PUFA-containing lipids; and (D) analysis of the characteristic differential n-3 PUFA-containing lipids.

cant upregulation (up), blue indicating significant downregulation (down), and grey indicating no significant difference (NS). Compared with the NanoE group, significantly upregulated lipids in the FLM-N group primarily included TG 54:10|18:2_16:3_20:5, TG 60:10|18:1_20:4_20:5, PC 38:7|18:2_20:5, DG 40:8|18:2_22:6, and PI 40:6|18:0_22:6. The SDG-N group exhibited primarily upregulated lipids including TG 58:13|18:3_20:5_20:5, TG 60:12|18:2_20:4_22:6, TG 62:15|20:4_20:5_22:6, and TG 62:16|20:5_20:5_22:6. The SECO-N group showed primarily upregulated lipids including TG 60:10|18:1_20:4_22:5, TG 62:15|20:4_20:5_22:6, PC 38:6|16:0_22:6, and PC 38:7|18:2_20:5. These results indicated differential regulatory effects of structurally distinct lignans on the metabolites derived from hepatic ALA conversion, wherein FLM and SECO may enhance hepatic synthesis and very low-density lipoprotein (VLDL)-associated secretion of ALA

conversion products in the form of TG and PC configurations, while SDG preferentially targets enhanced synthesis and secretion of TG-configured lipids.

Furthermore, integrating quantitative analysis of the characteristic differential n-3 PUFA-containing lipids (Fig. 5D) clarified the differentiated regulatory effects of co-administered lignans on serum lipid metabolism in mice. Compared with the Nano-E group, co-intake of FLM, SDG, or SECO all elevated specific n-3 PUFA-containing lipid configurations to varying degrees, exhibiting distinct differential characteristics. Specifically, for PC-class lipids, the FLM-N group significantly increased the levels of PC 38:7|18:2_20:5 configuration, suggesting FLM may promote EPA-associated PC lipid generation, whereas the SECO-N group significantly increased the levels of PC 38:6|16:0_22:6 configuration, indicating a potentially stronger role in promoting the syn-

thesis of DHA-containing PC lipids. Concerning TG-class lipids, all lignan-containing emulsions exhibited distinct promoting effects but with notable differences. The SDG-N group significantly increased multiple TG lipids including TG 56:9| 18:2_18:2_20:5, TG 58:13|18:3_20:5_20:5, TG 60:10| 18:1_20:4_22:5, TG 60:12|18:2_20:4_22:6, and TG 62:15| 20:4_20:5_22:6, indicating promoted synthesis of EPA- and DHA-featured TG configurations. The FLM-N group markedly upregulated specific TG configurations like TG 58:8|18:1_18:2_22:5 and TG 62:16|20:5_20:5_22:6, while the SECO-N group notably elevated levels of TG 56:9 and TG 58:8 lipids, showing clear advantages in promoting the synthesis of specific TG configurations. Collectively, co-administered FLM, SDG, and SECO nanoemulsions exerted differentiated regulatory effects on lipid synthesis pathways involving ALA metabolites, where FLM and SECO preferentially promoted conversion to PC and specific TG lipids, while SDG predominantly promoted TG lipid synthesis.

3.5. Hepatic metabolism analysis of flax lignans based on the nanoemulsion delivery system in mice

Previous *in vitro* gastrointestinal digestion and microbiota simulation experiments, as well as animal studies, showed that FLM exhibits high stability during the gastric digestion phase, with no significant structural changes observed. In the intestinal phase, limited hydrolysis of the FLM backbone structure occurs under digestive enzymes, releasing structural products such as SDG. Only a minimal portion is absorbed through the small intestine and reaches the liver *via* blood circulation, while the majority reaches the colon for further metabolism, with SDG deglycosylated to the aglycone SECO, followed by microbial metabolism into the absorbable metabolites END and ENL.[29]

In the current study, the differential metabolic pathways and hepatic accumulation of structurally different lignans were further investigated through single-dose gavage experiments in mice. Following pretreatment of the collected liver tissue, the content of flax lignans and their metabolites was quantitatively analyzed by LC-MS, and the representative chromatograms of the target compounds are shown in Fig. 6B. The results indicated that, as a polymeric macromolecule, FLM undergoes limited gastrointestinal depolymerization, releasing trace amounts of SDG, which can simultaneously be deglycosylated to SECO and reach the liver in the early absorption stage. The remaining components were metabolically depolymerized by the gut microbiota, with no SDG detected in the liver tissue,
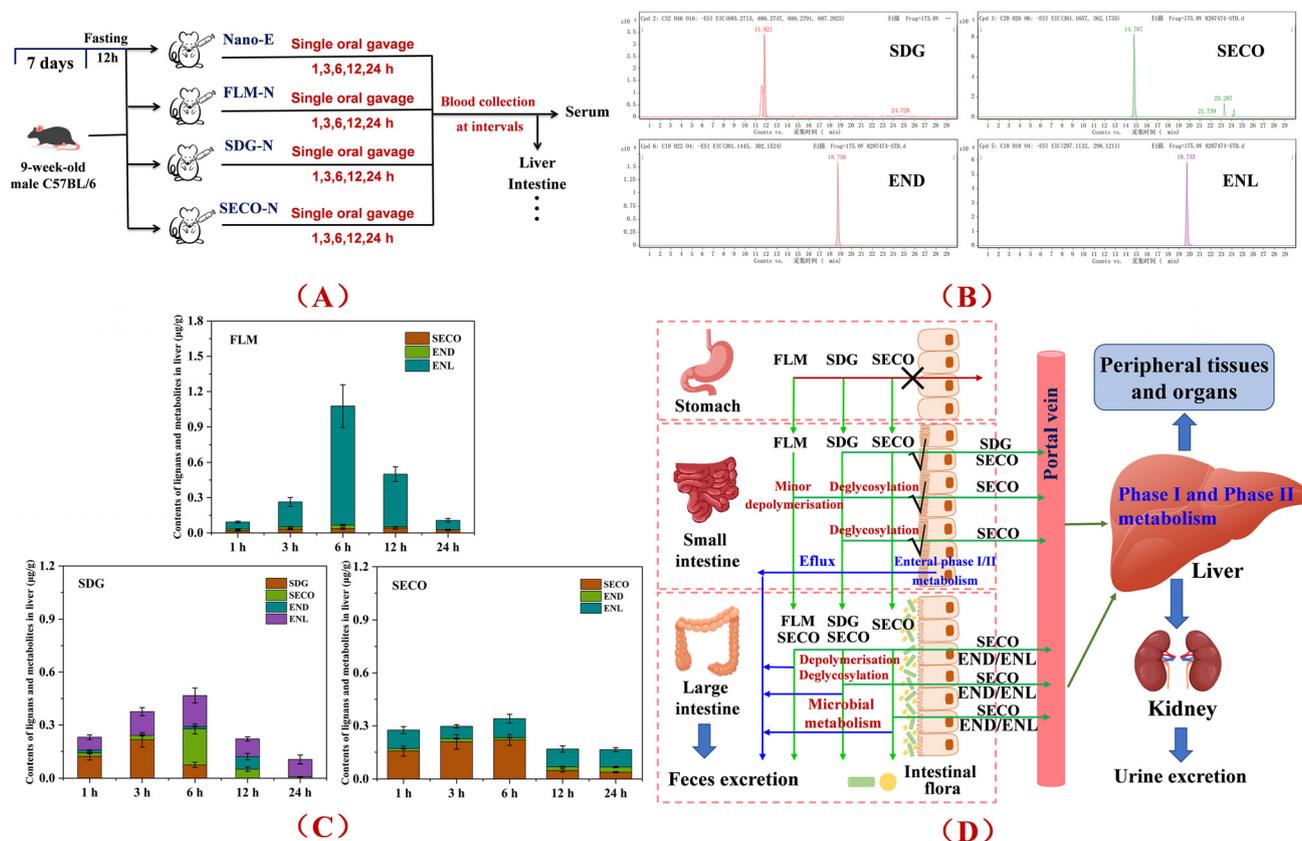

Fig. 6 Quantitative analysis of the characteristic metabolites of flax lignans in the nanoemulsion co-delivery systems in mice. (A) Experimental workflow of lignan metabolism in co-delivery emulsions; (B) chromatograms of the characteristic lignans and their metabolites; (C) quantitative analysis of the characteristic lignan metabolites in the mouse liver across the different emulsion groups; and (D) analysis of the differential metabolic pathways of different structural lignans.

indicating that depolymerization was accompanied by deglycosylation to form SECO, which was further metabolized to END and ENL (64.7%–93.8%) before reaching the liver. Generally, the release of natural molecular-form flax lignans during gastrointestinal digestion is extremely limited (1% or less), and only marginally influenced by intake forms.[41] Simultaneously, previous *in vitro* fermentation results showed a positive correlation between the released amount of SECO and its conversion rate to ENL. Microbiota is a key factor influencing colonic lignan metabolism, and adaptive modulation of the gut microbiota may increase plasma concentrations of the resultant enterolignans.[42]

Compared to FLM, the smaller molecular lignans, SDG and SECO, exhibited faster absorption, metabolism, and transport rates, reaching the liver rapidly *via* minor gastrointestinal absorption in the initial intake stage. For SDG, parent substrate levels existed in hepatic metabolites within 1–6 h (52.9%–57.5%–16.1%), while SECO generated *via* gastrointestinal enzymatic deglycosylation could be further absorbed, accounting for 6.8%–43.3%–23.0% of hepatic metabolites within 3–12 h. The remaining SDG was metabolized by the gut microbiota into END and ENL, further absorbed and transported to the liver, with ENL constituting 32.0%–45.2% of hepatic metabolites within 1–12 h. Previous studies reported detectable SDG in rat serum samples 0–12 h after high-dose SDG gavage, suggesting that SDG may enter the blood *via* direct absorption or lymphatic absorption followed by transfer into circulation, though specific mechanisms remain unclear.[43] Regarding SECO, rapid hepatic uptake occurred within 1 h post-administration, and parent SECO was present throughout the 1–24 h monitoring period (57.1%–70.3%–23.5%), while END and ENL formed by gut microbiota metabolism were concurrently absorbed into the liver, with ENL proportions ranging from 23.4%–59.1% during the monitoring period, as shown in Fig. 6C. Therefore, the current data indicate that structurally distinct flax lignans undergo differential metabolic pathways *in vivo* (Fig. 6D), with SDG, SECO, END, and ENL serving as the characteristic metabolites, providing an experimental basis for elucidating the material basis of hepatic metabolic conversion regulation.

Additionally, previous reports identified the presence of phase II metabolites such as SECO-Glu, END-Glu, and ENL-Glu in the sera and livers of mice fed lignan-containing diets.[35] In the current study, the differential generation of END-Sul, ENL-Glu, SECO-Sul, and SECO-Glu was observed across the lignan metabolism groups, although systematic quantification was not performed. Further research is warranted to explore the metabolic regulatory mechanisms and biological significance of these phase II metabolites.

3.6. Analysis of the co-incubation results of the characteristic flax lignan metabolites and ALA in HepG2 cells

Based on the *in vivo* metabolic results of structurally distinct flax lignans, the regulatory effects of the characteristic flax lignan metabolites on ALA metabolism *in vitro* were further investigated by HepG2 cell co-incubation experiments. Cells

were co-incubated for 48 h with non-cytotoxic concentrations of ALA and characteristic lignan metabolites. After incubation, the cells and the culture medium were separately collected for qualitative and quantitative fatty acid analyses. The results of intracellular fatty acid determination (Fig. 7A and B) showed that no chromatographic peaks for ALA or its conversion products were detected in the control group (without ALA). In the ALA-added group, chromatographic peaks for ALA and its conversion products (C20:3n-3 and C20:4n-3, ETA) were detected, indicating the intracellular conversion of ALA to ETA involving Δ6 desaturation and chain elongation processes. EPA and DHA contents were undetectable under the current co-incubation conditions, possibly due to low endogenous levels and minimal conversion rates of ALA metabolites within cells. Subsequently, quantitative analysis of intracellular ALA, C20:3n-3, and ETA revealed that, compared to the ALA control group, co-incubation with SDG, SECO, or END did not significantly alter the intracellular ALA content. However, co-incubation with ENL increased the intracellular ALA content by 23.1% ($p < 0.05$). Meanwhile, compared to the ALA control group, co-incubation with SDG decreased the intracellular 20:3 n-3 content by 11.8%, and co-incubation with END increased the C20:3n-3 content by 11.2%, though neither was significant. Notably, co-incubation with ENL increased the intracellular C20:3n-3 content by 48.6% ($p < 0.05$). Additionally, quantitative results for intracellular ETA showed a significant increase of 48.1% upon co-incubation with SDG ($p < 0.05$), while a non-significant increase of 9.2% was observed with SECO. However, ETA was undetectable within cells co-incubated with ENL.

Further quantitative analysis of fatty acids in the collected culture medium after incubation (Fig. 7C and D) showed that chromatographic peaks for ALA were detected in the media of all experimental groups except the blank control group, but no peaks for the ALA metabolic conversion products were observed. The quantitative results revealed no significant changes in the medium ALA content upon co-incubation with SDG and END compared with the ALA control group, indicating unaffected cellular transport of ALA. However, co-incubation with SECO or ENL significantly reduced ALA content in the medium ($p < 0.05$), with the SECO group showing a decrease by 10.2% and the ENL group by 40.1%, suggesting enhanced intracellular ALA uptake during co-incubation, consistent with the increased intracellular ALA content observed with ENL co-incubation. The non-significant change in the intracellular ALA content in the SECO group may imply enhanced metabolic conversion or increased fatty acid consumption due to cellular energy metabolism.

Integrative analysis of the medium ALA content and intracellular ALA and metabolite levels indicated that SDG does not affect cellular ALA uptake but promotes the simultaneous conversion of ALA to C20:3n-3 and ETA. SECO promotes cellular ALA uptake but had a limited effect on enhancing ALA conversion to ETA, possibly simultaneously enhancing intracellular ALA energy metabolism. END does not significantly influence ALA transport or metabolic conversion. ENL markedly
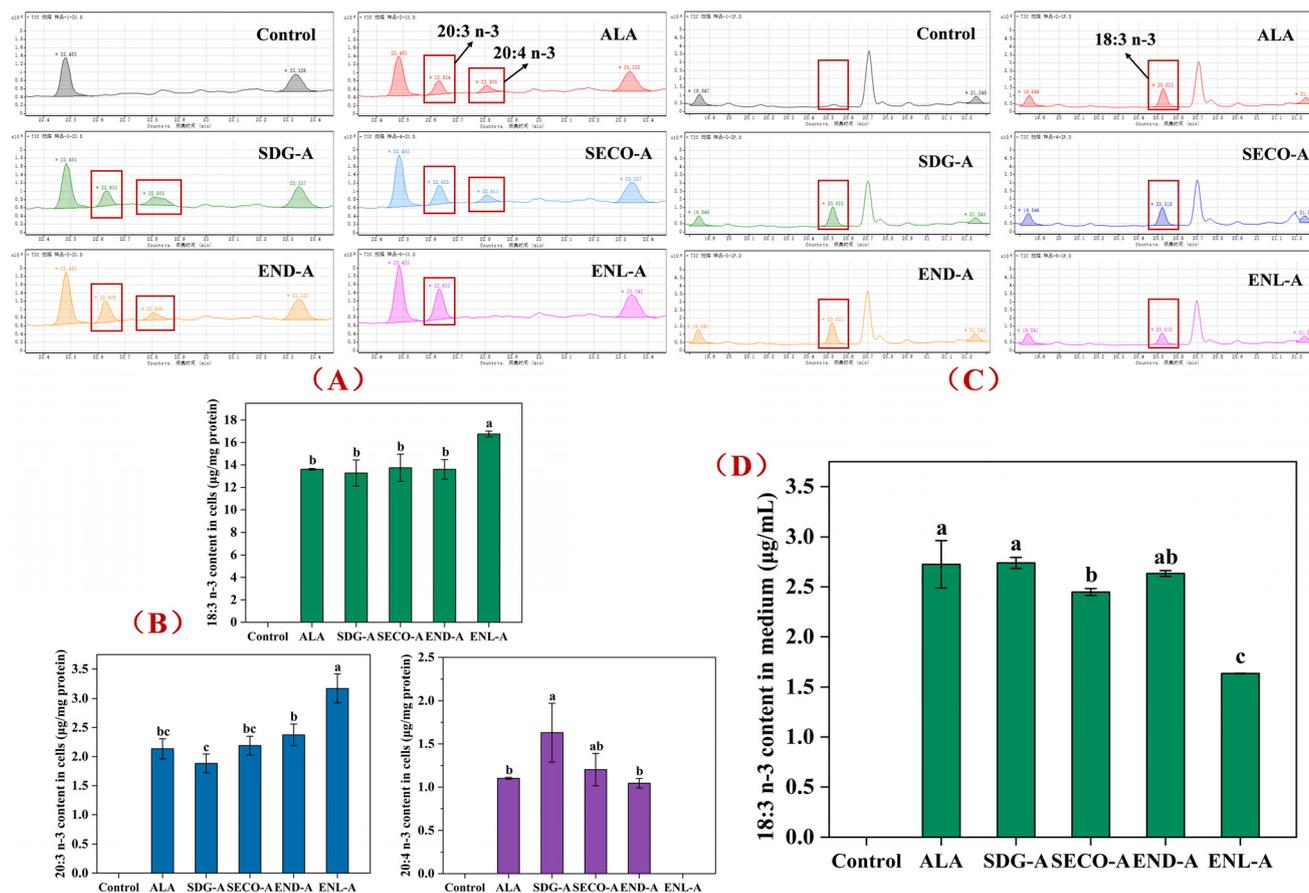
Fig. 7 Quantitative analysis of fatty acids in the intracellular and culture media following co-incubation of the characteristic lignan metabolites–ALA with HepG2 cells *in vitro*. (A) Chromatogram of the characteristic fatty acids in cells after co-incubation; (B) chromatogram of the characteristic fatty acids in the culture medium after co-incubation; (C) the intracellular concentrations of ALA, 20:3 n-3, and 20:4 n-3 (ETA); and (D) the concentration of ALA in the culture medium.

increases cellular ALA uptake and promotes conversion and accumulation to C20:3n-3, but may limit further metabolic conversion to ETA. Therefore, the current co-incubation results showed that the characteristic flax lignan metabolites differentially regulate ALA metabolism, potentially involving modulation of ALA transport, conversion, and metabolic pathways. SDG appears to be an effective material basis for regulating ALA metabolic conversion, while SECO and ENL may mediate ALA conversion regulation through multiple pathways, warranting further mechanistic investigation.

3.7. Potential regulatory effects of flax lignans on the hepatic metabolic conversion and secretory-circulation of ALA in nanoemulsions

Firstly, the gastrointestinal absorption, lymphatic transport, blood circulation, hepatic uptake, metabolism, and secretion pathways of ALA-containing lipids are illustrated (Fig. 8). CMs absorbed *via* intestinal uptake and lymphatic transport release fatty acids under the action of lipoprotein lipase (LPL) for peripheral uptake. Residual CM remnants are specifically recognized by hepatocytes and internalized through endocytosis,

followed by lysosomal degradation releasing free fatty acids (FFAs), including ALA.[44,45] Released ALA undergoes three primary metabolic pathways within hepatocytes: (1) participation in lipid resynthesis pathways leading to VLDL formation; (2) conversion into EPA, DPA, and DHA *via* desaturation and elongation processes mediated by the endoplasmic reticulum–Golgi apparatus system and peroxisomes; and (3) oxidation *via* mitochondrial β-oxidation pathways to supply the energy demands.[46] The dynamic process of intestinal absorption, lymph-blood transport, hepatic uptake, metabolism and secretion, and peripheral circulation and utilization of ALA-containing lipids presents challenges for precise quantification and evaluation of ALA metabolic conversion.

Based on multi-tissue dynamic monitoring and serum lipid configuration analysis, the current study assessed ALA metabolic conversion while analyzing the following potential mechanisms for lignan regulation of ALA metabolism: (1) flax lignans may alleviate product inhibition effects caused by long-term intake potentially by delaying the intestinal absorption–transport rate of ALA, thereby reducing the real-time hepatic metabolic load while facilitating gradual accumulation
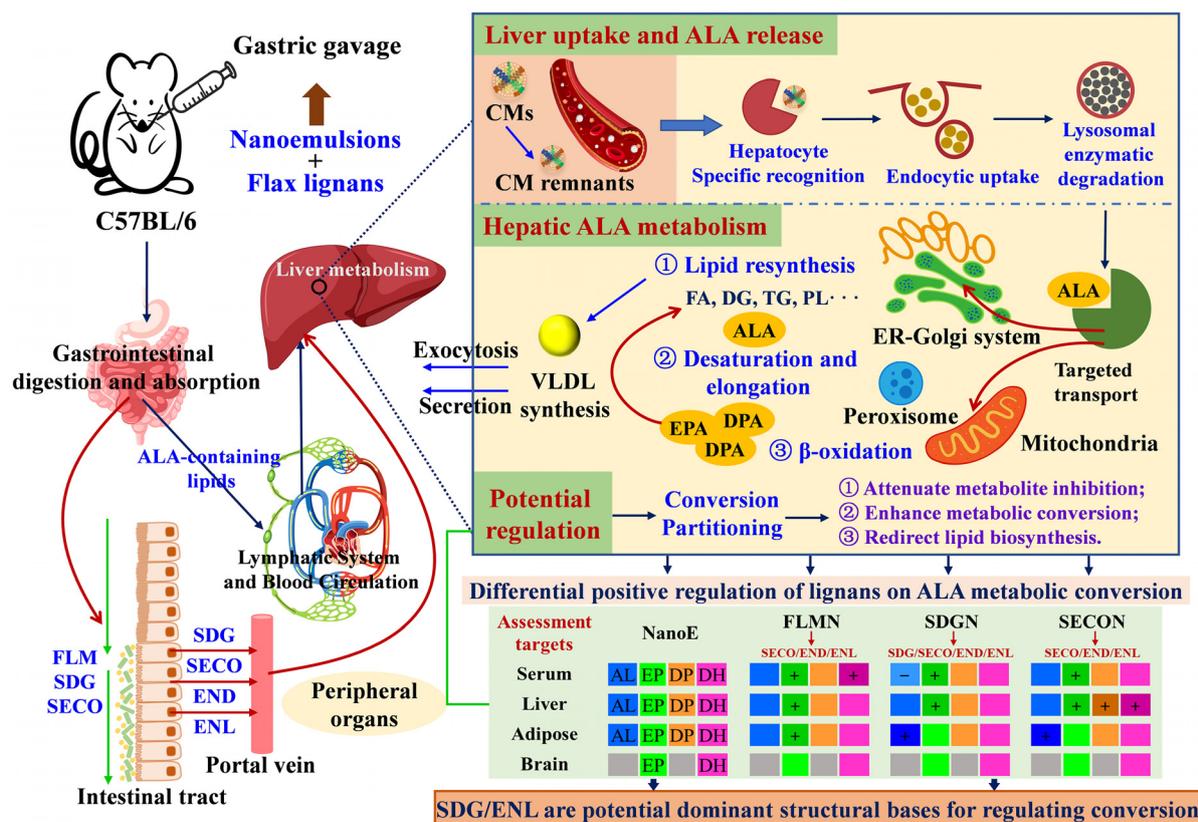
Fig. 8 Potential regulatory effects of flax lignans on the metabolic conversion of ALA to n-3 LCPUFAs based on the hepatic ALA uptake−conversion−secretion−recycling pathway.

of DPA and DHA; (2) flax lignans may exert potential differential regulatory effects on hepatic metabolic enzyme expression: FLM and SDG may preferentially enhance Δ6 desaturase-mediated DHA synthesis, whereas SECO may significantly improve EPA and DPA conversion efficiency by synergistically activating Δ5 desaturase and elongases; and (3) serum n-3 PUFA lipidomics revealed that lignans regulate metabolite distribution by remodeling lipid carrier configurations: FLM and SECO promoted incorporation of EPA/DHA into PC, whereas SDG specifically enriched EPA/DHA-containing TGs, suggesting enhanced peripheral delivery *via* lipoprotein secretion.

Therefore, flax lignans potentially achieve efficient synthesis and tissue-specific distribution of n-3 LCPUFAs through regulation of ALA absorption–metabolism dynamics, optimizing metabolic enzyme expression and remodeling lipid carriers. Simultaneously, integrating *in vivo* metabolic pathways and cell co-incubation experiments further elucidated potential mechanisms underlying ALA metabolic conversion regulated by structurally distinct flax lignans: (1) FLM is primarily metabolized to ENL through gastrointestinal depolymerization, deglycosylation, and microbial metabolism, providing the hepatic material basis, while smaller lignans (SDG and SECO) may directly enter the liver as parent compounds *via* absorption or transport, indicating that SDG, SECO, END, and ENL

could all exert potential regulatory roles, and (2) at the cellular metabolic level, ENL significantly promotes ALA cellular uptake and conversion/accumulation of intermediate products (C20:3n-3); SDG does not affect ALA absorption but significantly promotes ALA conversion to ETA, while SECO enhances cellular uptake of ALA but may promote ALA consumption toward energy metabolism pathways. Consequently, these differential mechanisms further show that the structural characteristics of flax lignans likely determine their material basis for gastrointestinal transport–hepatic metabolism, thereby influencing ALA absorption, transport, and conversion pathways, ultimately regulating n-3 fatty acid metabolic processes, with ENL and SDG potentially serving as key material bases for regulating ALA conversion to n-3 LCPUFAs.

Moreover, it should be specifically noted that the present investigation was conducted exclusively in male mice. However, potential sex differences in PUFA metabolism, particularly the conversion of ALA to n-3 LCPUFAs, warrant serious consideration. Accumulating evidence suggests that estrogen may modulate desaturation and elongation processes, potentially leading to greater synthesis of n-3 LCPUFAs in females. Furthermore, relatively lower rates of β-oxidation coupled with a greater propensity for lipid storage allocation in females may collectively favor the channeling of ALA towards n-3 LCPUFA synthesis over oxidative metabolism. These disparities likely originate from the

regulatory effects of sex hormones on the gene expression of key metabolic enzymes and overall lipid homeostasis.[2,47] Consequently, the generalizability of the enhancing effects of flax lignans on ALA conversion observed herein to females remains to be elucidated. Future studies employing both female and male animal models are imperative to comprehensively assess the potential sex-dependent responses to lignan supplementation and to clarify the underlying mechanisms. Such research is crucial for providing a more complete understanding of the nutritional implications of flax lignans across different human populations.

4. Conclusion

This study showed that co-intake of flax lignans (FLM, SDG and SECO) significantly enhanced the conversion of ALA to n-3 LCPUFAs in mice, exhibiting time-cumulative and tissue-specific regulatory effects. Lignan co-intake facilitated sustained accumulation of EPA, DPA, and DHA in the serum and liver, potentially by modulating ALA absorption rates and alleviating the hepatic metabolic load. FLM and SDG notably increased the serum DPA and DHA levels, while SECO synchronously elevated the hepatic EPA, DPA, and DHA contents, highlighting differential regulatory targets among distinct lignans. Lipidomic analyses revealed specific alterations in the serum lipid profiles. FLM and SECO promoted the incorporation of EPA/DHA into phospholipids, whereas SDG enriched EPA/DHA-containing triglycerides, suggesting enhanced n-3 LCPUFA delivery *via* lipoprotein secretion pathways. Notably, lignans exhibited minimal regulatory effects on the brain DHA, underscoring the blood–brain barrier's selective permeability. Consequently, further research is needed to clarify the molecular mechanisms underlying lignan-induced regulation of Δ5/Δ6 desaturase expression, the optimal dosage for long-term intake, and strategies to enhance DHA delivery across the blood–brain barrier. At the cellular level, ENL significantly enhanced the cellular uptake of ALA and promoted accumulation of its intermediate metabolite, C20:3n-3; SDG effectively promoted the further conversion of ALA to ETA, whereas SECO's regulation might involve cellular uptake combined with metabolic energy consumption. These findings suggest that ENL and SDG may serve as key material bases for regulating ALA conversion to n-3 LCPUFAs. Overall, flax lignans positively regulated ALA metabolic conversion through temporal orchestration of absorption–metabolism homeostasis, optimization of enzymatic reactions, and remodeling of lipid carriers. These findings provide valuable insights for nutritional strategies aimed at enhancing the bioavailability and metabolic conversion of ALA-based nanoemulsions.

Author contributions

Lei Wang: conceptualization, formal analysis, methodology, validation, visualization, and writing – original draft; Xiao Yu: conceptualization, data curation, and writing – review & editing; Chen Cheng: conceptualization and writing – review & editing; Jiqu Xu: conceptualization and writing – review & editing; Xia Xiang: conceptualization and writing – review & editing; Li Chen: conceptualization and writing – review & editing; Xiaoqiao Tang: conceptualization and writing – review & editing; and Qianchun Deng: conceptualization, funding acquisition, project administration, supervision, and writing – review & editing.

Conflicts of interest

The authors declare that they have no known competing financial interests or personal relationships that could have appeared to influence the work reported in this paper.

Abbreviations

ALA	α-Linolenic acid
N-3 LCPUFAs	N-3 long chain polyunsaturated fatty acids
FLM	Flax lignan macromolecule
SDG	Secoisolariciresinol diglucoside
SECO	Secoisolariciresinol
END	Enterodiol
ENL	Enterolactone
EPA	Eicosapentaenoic acid
DPA	Docosapentaenoic acid
DHA	Docosahexaenoic acid
PC	Phosphatidylcholine
TG	Triacylglycerol
CM	Chylomicron
FADS	Fatty acid desaturase
ELOVL	Elongase of very long chain fatty acid
VLDL	Very low-density lipoprotein

Data availability

The data supporting this article have been included as part of the supplementary information (SI). Supplementary information is available. See DOI: https://doi.org/10.1039/d5fo03469h.

Acknowledgements

References

1 I. Khan, M. Hussain, B. Jiang, L. Zheng, Y. Pan, J. Hu, A. Khan, A. Ashraf and X. Zou, Omega-3 long-chain polyunsaturated fatty acids: Metabolism and health implications, *Prog. Lipid Res.*, 2023, **92**, 101255, DOI: 10.1016/j.plipres.2023.101255.

2 R. H. M. de Groot, R. Emmett and B. J. Meyer, Non-dietary factors associated with n-3 long-chain PUFA levels in humans a systematic literature review, *Br. J. Nutr.*, 2019, **121**, 793–808, DOI: 10.1017/S0007114519000138.

3 K. Tan, H. Zhang and H. Zheng, Climate change and n-3 LC-PUFA availability, *Prog. Lipid Res.*, 2022, **86**, 101161, DOI: 10.1016/j.plipres.2022.101161.

4 D. Karnad, D. Gangadharan and Y. C. Krishna, Rethinking sustainability: From seafood consumption to seafood commons, *Geoforum*, 2021, **126**, 26–36, DOI: 10.1016/j.geoforum.2021.07.019.

5 S. S. Myers, M. R. Smith, S. Guth, C. D. Golden, B. Vaitla, N. D. Mueller, A. D. Dangour and P. Huybers, Climate change and global food systems: Potential impacts on food security and undernutrition, *Annu. Rev. Public Health*, 2017, **38**, 259–277, DOI: 10.1146/annurev-publhealth-031816-044356.

6 R. Micha, S. Khatibzadeh, P. Shi, S. Fahimi, S. Lim, K. G. Andrews, R. E. Engell, J. Powles, M. Ezzati and D. Mozaffarian, Global, regional, and national consumption levels of dietary fats and oils in 1990 and 2010: A systematic analysis including 266 country-specific nutrition surveys, *Br. Med. J.*, 2014, **348**, g2272, DOI: 10.1136/bmj.g2272.

7 G. C. Burdge, α-linolenic acid interconversion is sufficient as a source of longer chain ω-3 polyunsaturated fatty acids in humans: An opinion, *Lipids*, 2022, **57**, 267–287, DOI: 10.1002/lipd.12355.

8 S. Zhang, Y. Chen, D. J. McClements, T. Hou, F. Geng, P. Chen, H. Chen, B. Xie, Z. Sun, H. Tang, Y. Pei, S. Quan, X. Yu and Q. Deng, Composition, processing, and quality control of whole flaxseed products used to fortify foods, *Compr. Rev. Food Sci. Food Saf.*, 2023, **22**, 587–614, DOI: 10.1111/1541-4337.13086.

9 L. Wang, C. Cheng, X. Yu, L. Guo, X. Wan, J. Xu, X. Xiang, J. Yang, J. Kang and Q. Deng, Conversion of α-linolenic acid into n-3 long-chain polyunsaturated fatty acids: Bioavailability and dietary regulation, *Crit. Rev. Food Sci. Nutr.*, 2025, **65**, 6470–6502, DOI: 10.1080/10408398.2024.2442064.

10 L. A. Videla, M. C. Hernandez-Rodas, A. H. Metherel and R. Valenzuela, Influence of the nutritional status and oxidative stress in the desaturation and elongation of n-3 and n-6 polyunsaturated fatty acids: Impact on non-alcoholic fatty liver disease, *Prostaglandins, Leukotrienes Essent. Fatty Acids*, 2022, **181**, 102441, DOI: 10.1016/j.plefa.2022.102441.

11 R. Valenzuela, A. H. Metherel, G. Cisbani, M. E. Smith, R. Chouinard-Watkins, B. J. Klievik, L. A. Videla and R. P. Bazinet, Protein concentrations and activities of fatty acid desaturase and elongase enzymes in liver, brain, testicle, and kidney from mice: Substrate dependency, *BioFactors*, 2023, **50**, 89–100, DOI: 10.1002/biof.1992.

12 R. Valenzuela, A. H. Metherel, G. Cisbani, M. E. Smith, R. Chouinard-Watkins, B. J. Klievik, C. Farias, L. A. Videla and R. P. Bazinet, Specific activity of mouse liver desaturases and elongases: Time course effects using n-3 and n-6 PUFA substrates and inhibitory responses of delta-6 desaturase, *Biochim. Biophys. Acta, Mol. Cell Biol. Lipids*, 2025, **1870**, 159594, DOI: 10.1016/j.bbalip.2025.159594.

13 R. D. Rotarescu, M. Mathur, A. M. Bejoy, G. H. Anderson and A. H. Metherel, Serum measures of docosahexaenoic acid (DHA) synthesis underestimates whole body DHA synthesis in male and female mice, *J. Nutr. Biochem.*, 2024, **131**, 109689, DOI: 10.1016/j.jnutbio.2024.109689.

14 L. Couëdelo, S. Amara, M. Lecomte, E. Meugnier, J. Monteil, L. Fonseca, G. Pineau, M. Cansell, F. Carrière, M. C. Michalski and C. Vaysse, Impact of various emulsifiers on ALA bioavailability and chylomicron synthesis through changes in gastrointestinal lipolysis, *Food Funct.*, 2015, **6**, 1726–1735, DOI: 10.1039/C5FO00070J.

15 C. C. Berton-Carabin, M. H. Ropers and C. Genot, Lipid oxidation in oil-in-water emulsions: Involvement of the interfacial layer, *Compr. Rev. Food Sci. Food Saf.*, 2014, **13**, 945–977, DOI: 10.1111/1541-4337.12097.

16 D. Sugasini and B. R. Lokesh, Curcumin and linseed oil co-delivered in phospholipid nanoemulsions enhances the levels of docosahexaenoic acid in serum and tissue lipids of rats, *Prostaglandins, Leukotrienes Essent. Fatty Acids*, 2017, **119**, 45–52, DOI: 10.1016/j.plefa.2017.03.007.

17 A. Wu, E. E. Noble, E. Tyagi, Z. Ying, Y. Zhuang and F. Gomez-Pinilla, Curcumin boosts DHA in the brain: Implications for the prevention of anxiety disorders, *Biochim. Biophys. Acta, Mol. Basis Dis.*, 2015, **1852**, 951–961, DOI: 10.1016/j.bbadis.2014.12.005.

18 G. Kühn, K. Pallauf, C. Schulz, M. Birringer, B. Diaz-Rica, S. de Pascual-Teresa and G. Rimbach, Resveratrol modulates desaturase expression and fatty acid composition of cultured hepatocytes, *Front. Nutr.*, 2018, **5**, 106, DOI: 10.3389/fnut.2018.00106.

19 S. Trattner, B. Ruyter, T. K. Østbye, T. Gjøen, V. Zlabek, A. Kamal-Eldin and J. Pickova, Sesamin increases alpha-linolenic acid conversion to docosahexaenoic acid in Atlantic salmon (Salmo salar L.) hepatocytes: Role of altered gene expression, *Lipids*, 2008, **43**, 999–1008, DOI: 10.1007/s11745-008-3229-7.

20 S. Trattner, A. Kamal-Eldin, E. Brännäs, A. Moazzami, V. Zlabek, P. Larsson, B. Ruyter, T. Gjøen and J. Pickova, Sesamin supplementation increases white muscle docosahexaenoic acid (DHA) levels in rainbow trout (Oncorhynchus mykiss) fed high alpha-linolenic acid (ALA) containing vegetable oil: Metabolic actions, *Lipids*, 2008, **43**, 989–997, DOI: 10.1007/s11745-008-3228-8.

21 J. Mellery, F. Scalisi, C. Bonnineau, P. Kestemont, X. Rollin and Y. Larondelle, Impact of lignans on the polyunsaturated fatty acid metabolic processing in a rainbow trout

(Oncorhynchus mykiss) cell line, *Aquaculture*, 2017, **476**, 106–110, DOI: 10.1016/j.aquaculture.2017.04.022.

22 K. Drygalski, K. Berk, T. Charytoniuk, N. Iłowska, B. Łukaszuk, A. Chabowski and K. Konstantynowicz-Nowicka, Does the enterolactone (ENL) affect fatty acid transporters and lipid metabolism in liver?, *Nutr. Metab.*, 2017, **14**, 69, DOI: 10.1186/s12986-017-0223-1.

23 C. Burak, S. Wolffram, B. Zur, P. Langguth, R. Fimmers, B. Alteheld, P. Stehle and S. Egert, Effects of the flavonol quercetin and α-linolenic acid on n-3 PUFA status in metabolically healthy men and women: a randomised, double-blinded, placebo-controlled, crossover trial, *Br. J. Nutr.*, 2017, **117**, 698–711, DOI: 10.1017/S0007114517000241.

24 M. Wu, H. Su, Y. Cui, A. Windust, H. Chou and C. Huang, Fucoxanthin enhances chain elongation and desaturation of alpha-linolenic acid in HepG2 cells, *Lipids*, 2015, **50**, 945–953, DOI: 10.1007/s11745-015-4059-z.

25 X. Y. Li, T. X. Yang, Y. C. Zhao, C. C. Wang, C. H. Xue, T. Yanagita, Y. M. Wang and T. T. Zhang, Fucoxanthin promotes the chain lengthening reaction of polyunsaturated fatty acids *in vivo* by enhancing FADS2 enzyme activity, *Food Sci. Hum. Wellness*, 2025, **14**, 9250130, DOI: 10.26599/FSHW.2024.9250130.

26 D. Vauzour, N. Tejera, C. O'Neill, V. Booz, B. Jude, I. M. A. Wolf, N. Rigby, J. M. Silvan, P. J. Curtis, A. Cassidy, S. de Pascual-Teresa, G. Rimbach and A. M. Minihane, Anthocyanins do not influence long-chain n-3 fatty acid status: Studies in cells, rodents and humans, *J. Nutr. Biochem.*, 2015, **26**, 211–218, DOI: 10.1016/j.jnutbio.2014.09.005.

27 M. Saleem, H. J. Kim, M. S. Ali and Y. S. Lee, An update on bioactive plant lignans, *Nat. Prod. Rep.*, 2005, **22**, 696–716, DOI: 10.1039/B514045P.

28 A. Kamal-Eldin, N. Peerlkamp, P. Johnsson, R. Andersson, R. E. Andersson, L. N. Lundgren and P. Åman, An oligomer from flaxseed composed of secoisolariciresinoldiglucoside and 3-hydroxy-3-methyl glutaric acid residues, *Phytochemistry*, 2001, **58**, 587–590, DOI: 10.1016/S0031-9422(01)00279-5.

29 E. Eeckhaut, K. Struijs, S. Possemiers, J. P. Vincken, D. D. Keukeleire and W. Verstraete, Metabolism of the lignan macromolecule into enterolignans in the gastrointestinal lumen as determined in the simulator of the human intestinal microbial ecosystem, *J. Agric. Food Chem.*, 2008, **56**, 4806–4812, DOI: 10.1021/jf800101s.

30 C. Cheng, X. Yu, F. Huang, D. Peng, H. Chen, Y. Chen, Q. Huang and Q. Deng, Effect of different structural flaxseed lignans on the stability of flaxseed oil-in-water emulsion: An interfacial perspective, *Food Chem.*, 2021, **357**, 129522, DOI: 10.1016/j.foodchem.2021.129522.

31 L. Wang, X. Yu, C. Cheng, J. Xu, X. Xiang, L. Chen, X. Tang, X. Wang and Q. Deng, Flax lignans modulate the digestion and absorption of α-linolenic acid in sunflower phospholipid-stabilized nanoemulsions: *In vitro* digestion simulation and *in vivo* studies in mice, *Food Res. Int.*, 2025, **220**, 117049, DOI: 10.1016/j.foodres.2025.117049.

32 L. Wang, X. Yu, C. Cheng, J. Xu, X. Xiang, X. Tang and Q. Deng, Flax lignans regulate the conversion of α-linolenic acid into n-3 LCPUFAs in mice ingesting sunflower phospholipid-stabilized nanoemulsions, *Food Sci. Hum. Wellness*, 2025, **14**, 9250371, DOI: 10.26599/FSHW.2024.9250371.

33 E. G. Dyer and W. J. Bligh, A rapid method of total lipid extraction and purification, *Can. J. Biochem. Physiol.*, 1959, **37**, 911–917, DOI: 10.1139/o59-099.

34 J. Wang, X. Yu, S. Ran and F. Wei, Comprehensive lipid profile analysis of three fish roe by untargeted lipidomics using ultraperformance liquid chromatography coupled with quadrupole time-of-flight tandem mass spectrometry, *J. Food Compos. Anal.*, 2024, **136**, 106782, DOI: 10.1016/j.jfca.2024.106782.

35 D. García-Mateos, R. García-Villalba, J. A. Otero, J. A. Marañón, J. C. Espín, A. I. Álvarez and G. Merino, An altered tissue distribution of flaxseed lignans and their metabolites in Abcg2 knockout mice, *Food Funct.*, 2018, **9**, 636–642, DOI: 10.1039/C7FO01549F.

36 S. Bolca, M. Urpi-Sarda, P. Blondeel, N. Roche, L. Vanhaecke, S. Possemiers, N. Al-Maharik, N. Botting, D. De Keukeleire, M. Bracke, A. Heyerick, C. Manach and H. Depypere, Disposition of soy isoflavones in normal human breast tissue, *Am. J. Clin. Nutr.*, 2010, **91**, 976–984, DOI: 10.3945/ajcn.2009.28854.

37 R. Alhazzaa, A. J. Sinclair and G. M. Turchini, Bioconversion of α-linolenic acid into n-3 long-chain polyunsaturated fatty acid in Hepatocytes and Ad Hoc cell culture optimisation, *PLoS One*, 2013, **8**, e73719, DOI: 10.1371/journal.pone.0073719.

38 H. R. Martínez-Ramírez, J. P. Cant, A. K. Shoveller, J. L. Atkinson and C. F. M. de Lange, Whole-body retention of α-linolenic acid and its apparent conversion to other n-3 PUFA in growing pigs are reduced with the duration of feeding α-linolenic acid, *Br. J. Nutr.*, 2014, **111**, 1382–1393, DOI: 10.1017/S0007114513003991.

39 S. Wang, Y. Pan, J. Li, H. Chen, H. Zhang, W. Chen, Z. Gu and Y. Q. Chen, Endogenous omega-3 long-chain fatty acid biosynthesis from alpha-linolenic acid is affected by substrate levels, gene expression, and product inhibition, *RSC Adv.*, 2017, **7**, 40946–40951, DOI: 10.1039/C7RA06728C.

40 R. Valenzuela, C. Barrera, J. M. Ayala, J. Sanhueza and A. Valenzuela, Vegetable oils rich in alpha linolenic acid allow a higher accretion of n-3 LCPUFA in the plasma, liver and adipose tissue of the rat, *Grasas Aceites*, 2014, **65**, e026, DOI: 10.3989/gya.110113.

41 C. Fuentealba, F. Figuerola, A. M. Estévez, J. M. Bastías and O. Muñoz, Bioaccessibility of lignans from flaxseed (Linum usitatissimum L.) determined by single-batch *in vitro* simulation of the digestive process, *J. Sci. Food Agric.*, 2014, **94**, 1729–1738, DOI: 10.1002/jsfa.6482.

42 U. K. H. Zaki, C. Fryganas, L. Trijsburg, E. J. M. Feskens and E. Capuano, *In vitro* gastrointestinal bioaccessibility and colonic fermentation of lignans from fresh, fermented,

and germinated flaxseed, *Food Funct.*, 2022, **13**, 10737–10747, DOI: 10.1039/D2FO02559K.

43 W. Zhou, G. Wang and Z. Han, The metabolism of flaxseed lignans in rats, *Acta Vet. Zootech. Sin.*, 2009, **40**, 763–768.

44 S. Dash, C. Xiao, C. Morgantini and G. F. Lewis, New insights into the regulation of chylomicron production, *Annu. Rev. Nutr.*, 2015, **35**, 265–294, DOI: 10.1146/annurev-nutr-071714-034338.

45 A. L. Jones, G. T. Hradek, C. Hornick, G. Renaud, E. E. T. Windler and R. J. Havel, Uptake and processing of remnants of chylomicrons and very low density lipopro-teins by rat liver, *J. Lipid Res.*, 1984, **25**, 1151–1158, DOI: 10.1089/jir.1984.4.635.

46 G. Barceló-Coblijn and E. J. Murphy, Alpha-linolenic acid and its conversion to longer chain n-3 fatty acids: Benefits for human health and a role in maintaining tissue n-3 fatty acid levels, *Prog. Lipid Res.*, 2009, **48**, 355–374, DOI: 10.1016/j.plipres.2009.07.002.

47 E. J. Baker, E. A. Miles, G. C. Burdge, P. Yaqoob and P. C. Calder, Metabolism and functional effects of plant-derived omega-3 fatty acids in humans, *Prog. Lipid Res.*, 2016, **64**, 30–56, DOI: 10.1016/j.plipres.2016.07.002.